Rivista Italiana di Paleontologia e Stratigrafia
(*Research in Paleontology and Stratigraphy*)
vol. 129(1): 1-24. **March 2023**
DOI: https://doi.org/10.54103/2039-4942/17938

RECONSTRUCTING KUNGURIAN (CISURALIAN, PERMIAN) TERRESTRIAL ENVIRONMENTS WITHIN A MEGACALDERA IN THE SOUTHERN ALPS (N-ITALY) USING LITHOFACIES ANALYSIS, PALYNOLOGY AND STABLE CARBON ISOTOPES

FRANCESCA VALLÉ[1*], HENDRIK NOWAK[1], EVELYN KUSTATSCHER[1,2,3], SALLY ERKENS[1,4], GUIDO ROGHI[5], CORRADO MORELLI[6], KARL KRAINER[7], NEREO PRETO[8] & CHRISTOPH HARTKOPF-FRÖDER[9]

[1]Museum of Nature South Tyrol, Bindergasse/Via Bottai 1, 39100 Bozen/Bolzano, Italy. E-mail: Hendrik.Nowak@naturmuseum.it; Evelyn.Kustatscher@naturmuseum.it
[2]Department of Earth and Environmental Sciences, Palaeontology & Geobiology, Ludwig-Maximilians-Universität München, Richard-Wagner-Straße 10, 80333 München, Germany.
[3]SNSB-Bayerische Staatssammlung für Paläontologie und Geologie, Richard-Wagner-Straße 10, 80333 München, Germany.
[4]Institute of Earth and Environmental Sciences, University of Freiburg, Tennenbacher Str. 4, 79106 Freiburg, Germany. E-mail: sally.erkens@gmail.com
[5]Institute of Geosciences and Earth Resources - CNR, Via Gradenigo 6, 35131Padova, Italy. E-mail: guido.roghi@igg.cnr.it
[6]Ufficio Geologia e Prove Materiali, Provincia Autonoma di Bolzano, Via Val d'Ega, 48, 39053 Kardaun/Cardano, Italy. E-mail: Corrado.Morelli@provinz.bz.it
[7]Institute of Geology, University of Innsbruck, Innrain 52, 6020 Innsbruck, Austria. E-mail: Karl.Krainer@uibk.ac.at
[8]Department of Geosciences, University of Padua, Via Gradenigo 6, 35131 Padova, Italy. E-mail: nereo.preto@unipd.it
[9]Institute of Geology and Mineralogy, University of Cologne, Zülpicher Str. 49a, 50674 Köln, Germany. E-mail: hartkopf-froeder@gmx.de
*Corresponding Author: francescavalle83@gmail.com

Associate Editor: Lucia Angiolini.

To cite this article: Vallé F., Nowak H., Kustatscher E., Erkens S., Roghi G., Morelli C., Krainer K., Preto N. & Hartkopf-Fröder C. (2023) - Reconstructing Kungurian (Cisuralian, Permian) terrestrial environments within a megacaldera in the Southern Alps (N-Italy) using lithofacies analysis, palynology and stable carbon isotopes. *Riv. It. Paleontol. Strat.*, 129(1): 1-24.

Keywords: Early Permian; palynofacies; sporomorphs; depositional environments; sedimentology; vegetation.

Abstract. During the Permian, climate experienced a change from icehouse to greenhouse conditions. Few multidisciplinary studies have investigated Kungurian (late Cisuralian) tropical terrestrial ecosystem and climate changes. Here, we apply an interdisciplinary approach to two alluvial-lacustrine successions of the Athesian Volcanic Group (Southern Alps, northern Italy) deposited in a Kungurian megacaldera during periods of volcanic quiescence. Sedimentological analysis combined with palynofacies studies allowed the reconstruction of the depositional environments. The study of sporomorph assemblages and stable organic carbon isotopes provided information on plant communities and the climate context. Two different depositional environments were present in the megacaldera: one proximal and one more distal with respect to the source, distinguished by a slightly different composition of the sediments, palynofacies and organic carbon isotopes. The plant community in the area was dominated by xeromorphic-hygromorphic taxa. The $\delta^{13}C_{org}$ values are comparable to those of other Cisuralian continental organic matter and plants. The stable carbon isotope values show a small variability, which correlates weakly, but significantly, with the abundance of xeromorphic elements. All observations support deposition during semiarid to arid climate conditions, typical of the mid-late Cisuralian in the area.

Received: May 23, 2022; accepted: September 30, 2022

Introduction

The late Palaeozoic was a time of important changes in palaeogeography, climate and composition of the terrestrial ecosystems. The Late Palaeozoic Ice Age (LPIA), the longest ice age of the Phanerozoic (~335-256 Ma; e.g., Montañez et al. 2007; Isbell et al. 2021; Montañez 2022), reached its apex during the Cisuralian with the formation of widespread continental ice sheets (e.g., Frakes et al. 1992; Isbell et al. 2003; Jones & Fielding 2004; Montañez et al. 2007; Montañez & Poulsen 2013). The eccentricity-scaled glacial-interglacial cycles produced large fluctuations of sea level (e.g., Rankey 1997; Olszewski & Patzkowsky 2003) and consequently palaeogeographical and palaeoenvironmental changes. Within these climate dynamics, the Earth experienced a change from icehouse to greenhouse conditions (e.g., Montañez et al. 2007; Montañez & Poulsen 2013; Montañez et al. 2016) as a consequence of changes in the atmospheric pCO_2 and related responses from the oceans, the wind systems (e.g., Montañez & Poulsen 2013), precipitation (e.g., DiMichele et al. 2008; Montañez & Poulsen 2013), and vegetation (e.g., Montañez et al. 2016).

At low latitudes, a stepwise aridification trend, interrupted by wetter intervals (e.g., Roscher & Schneider 2006; DiMichele et al. 2008, 2009), started in the Late Pennsylvanian (e.g., Schneider et al. 2006; DiMichele et al. 2008, 2009; Montañez et al. 2016; Bashforth et al. 2021) and continued until the Late Triassic (e.g., Schneider et al. 2020). This led to changes in the composition of the tropical Euramerican floras and in biome distributions during the Permian (e.g., DiMichele et al. 2008; Bashforth et al. 2021), from dominant wetland to dryland biomes (Bashforth et al. 2021). As shown recently by Marchetti et al. (2022), a dramatic increase in both diversity and relative abundance of drought-tolerant taxa took place in central Pangaea during the Artinskian, at about 287 Ma. This biotic replacement was sudden, conspicuous, widespread, and time-equivalent to the biotic replacement observed at the low palaeolatitudes of western Pangaea and to a major increase of pCO_2 and Na_2O values evident in Euramerican successions (Marchetti et al. 2022). These changes in global climate conditions are reflected in the qualitative and quantitative composition of the plant communities and in the isotope composition of the plant remains. The $\delta^{13}C_{org}$ (stable carbon isotope composition of organic matter) of Cisuralian terrestrial plants fluctuated around -22‰ - which is rather heavy with respect to the rest of the Phanerozoic, increased during the Cisuralian and decreased significantly in the Lopingian (e.g., Dong et al. 2021).

Few multidisciplinary studies have investigated Cisuralian tropical terrestrial ecosystem and climate changes. One of the reference areas for the study of terrestrial ecosystems at low latitudes during the Cisuralian lies in the Southern Alps in northern Italy. The Athesian Volcanic Group (AG) formed by the explosive activity of a megacaldera during 289-274 Ma, approximately equivalent to the Artinskian-Kungurian (e.g., Marocchi et al. 2008; Morelli et al. 2012). Intercalated in the volcanic units, sedimentary rocks were deposited during periods of volcanic quiescence. Some of these epiclastic units (i.e., in the Tregiovo Basin) are age-constrained by radiometric dating in the under- and overlying volcanic unit and are well-known for their abundant plant macro- and microfossils as well as vertebrate and invertebrate remains and vertebrate traces (e.g., Cassinis & Doubinger 1991, 1992; Cassinis & Neri 1992; Barth & Mohr 1994; Neri et al. 1999; Visscher et al. 2001; Avanzini et al. 2011; Forte et al. 2017; Marchetti et al. 2017; Forte et al. 2018a). However, only few studies integrate the different terrestrial ecosystem components to reconstruct palaeoenvironments and climate changes (Marchetti et al. 2015, 2022; Forte et al. 2018b). In combination with sedimentological analyses, the study of the sedimentary organic matter particles (palynofacies analysis) is considered a useful tool to reconstruct palaeoenvironments and depositional settings both in marine (e.g., Tyson 1993, 1995; Batten 1996) and terrestrial settings (e.g., Batten 1996; Martín-Closas et al. 2005; Müller et al. 2006; Cirilli et al. 2018; Aggarwal 2021; Spina et al. 2021).

In this study, we use an interdisciplinary approach (lithofacies, palynofacies and stable carbon isotopes analyses) on two alluvial and lacustrine successions of the same Kungurian epiclastic intercalation (Guntschna/Guncina Formation) to define the depositional environments developed within a sedimentary basin in the megacaldera. The systematic quantitative and qualitative study of the

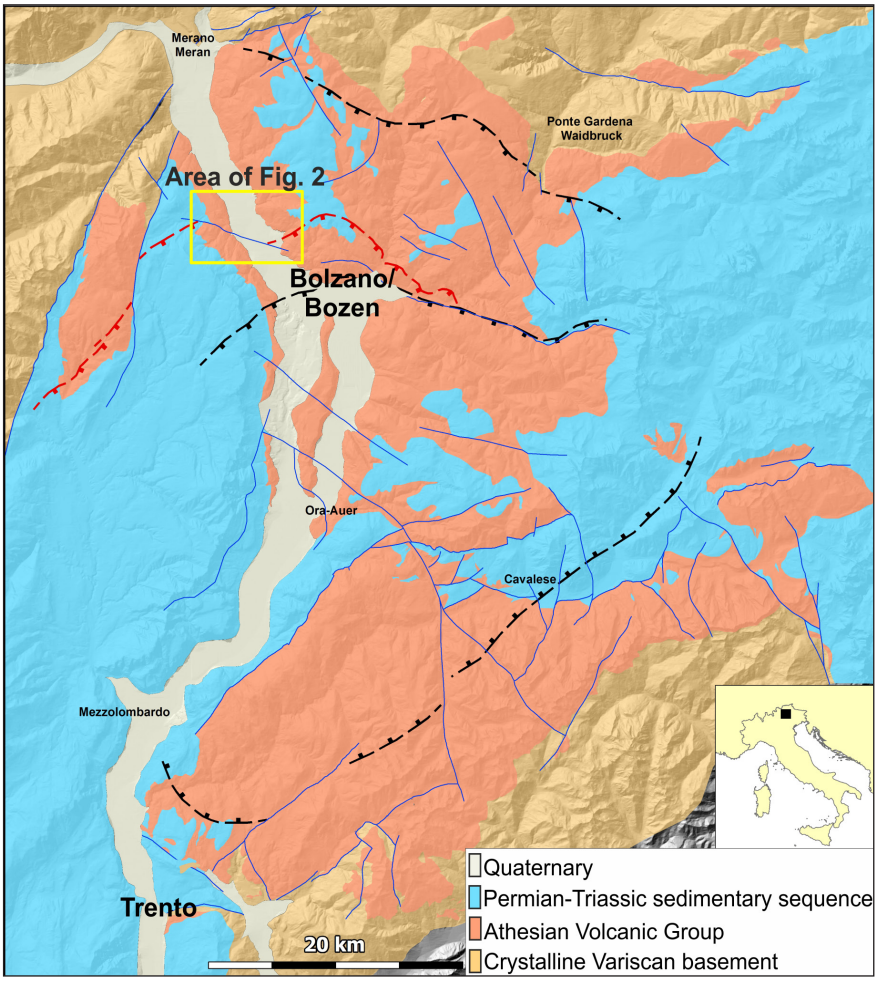

Fig. 1 - Simplified geological map showing the location of the studied area. Blue lines are Alpine faults. The black lines are caldera collapses and the red ones a synvolcanic collapse related to postcaldera resurgence.

sporomorphs (pollen and spores), the association to their parent plants (or plant groups) and the inferred plant ecoclimatic preferences (xeromorphic, xeromorphic-hygromorphic, hygromorphic) allow us to reconstruct the changes in vegetation and local climate conditions throughout the sections. A comparison between the relative abundance of the various sporomorph groups and the $\delta^{13}C_{org}$ of bulk rock underscores the influence of local and possibly large-scale factors on vegetational composition and deposition of organic matter at different positions in such a caldera system.

Geological setting

The Athesian Volcanic Group (AG) crops out over an area of more than 2000 square kilometres between the provinces of Bozen/Bolzano and Trento (Fig. 1), making it one of the largest and best-exposed areas of Permian volcanic rocks in Europe. The AG includes both volcanic and continental sedimentary rocks. They constitute a more than 4000 m thick succession, which formed during the Cisuralian in a post-orogenic extensional geodynamic context. The onset of the different stratigraphic units was strongly influenced by extensive synvolcanic tectonic processes related to the development of wide calderas of different ages. Generally, the collapses are getting younger towards the centre of the volcanic system meaning that parts of the younger successions were deposited not on top but laterally to the older ones in the spaces created by calderic collapses. The AG volcanic activity lasted about 15 Myr during part of the Cisuralian (~289-274 Ma) with a deposition rate that increased throughout the eruptive cycle (Schaltegger & Brack 2007; Visonà et al. 2007; Marocchi et al. 2008; Morelli et al. 2007, 2012; Brandner et al. 2016).

The magmatic activity in the early phases of the caldera was dominated by lava flows, mainly andesites to rhyodacites in composition. During the intermediate to late stages the main activi-

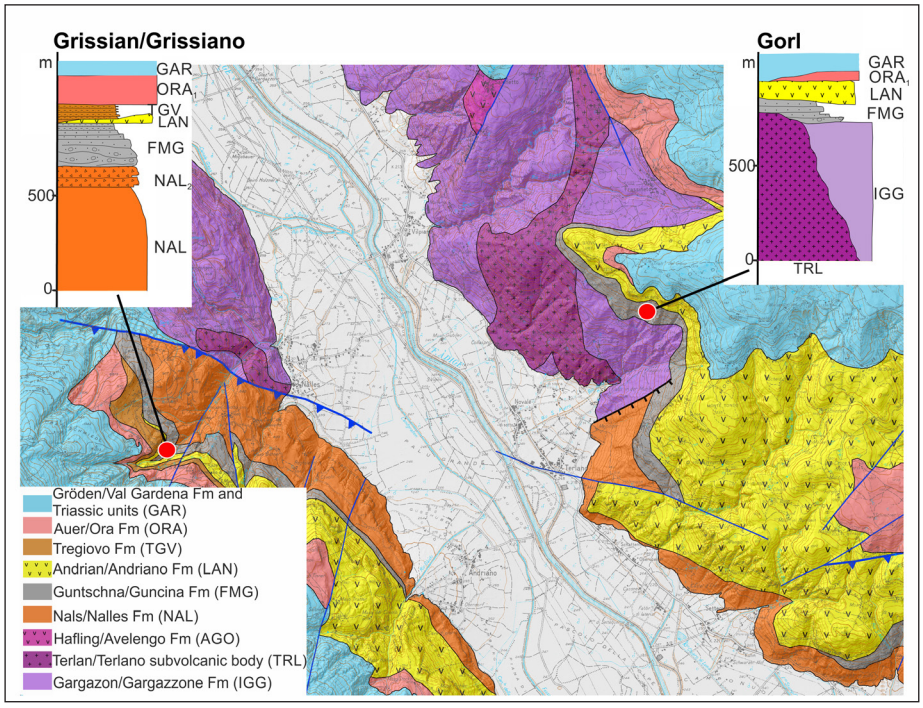

Fig. 2 - Geological map of the studied area with the stratigraphic logs of the investigated sections. The units in the map have the same colours as in the logs: IGG - Gargazon/Gargazzone Formation, TRL - Terlan/Terlano Subvolcano body, FMG - Guntschna/Guncina Formation, LAN - Andrian/Andriano Formation, ORA_1 - Perdonig/Predonico Member of the Auer/Ora Formation, NAL - Nals/Nalles Formation, NAL_2 - San Cosma e Damiano Member of the Nals/Nalles Formation, TGV - Tregiovo Formation, GAR - Gröden/Val Gardena Formation. Red dots indicate the locations of the investigated sections.

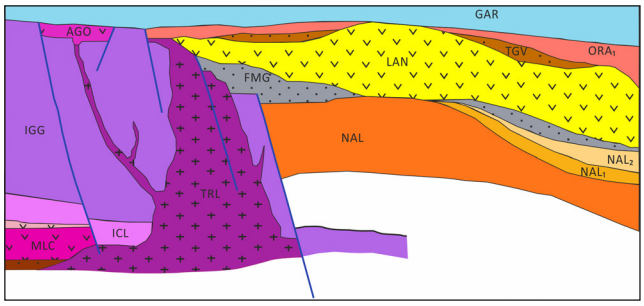

Fig. 3 - Schematic stratigraphic section in an approximately north-south direction to show the geometric relationship of the Guntschna/Guncina Formation with the other stratigraphic units of the AG. MLC - Laugen/Monte Luco Formation, ICL - Leonburg/Castel Leone Formation, IGG - Gargazon/Gargazzone Formation, TRL - Terlan/Terlano Subvolcano body, AGO - Hafling/Avelengo Formation, FMG - Guntschna/Guncina Formation, LAN - Andrian/Andriano Formation, NAL - Nals/Nalles Formation, NAL_1 - San Maurizio Member of the Nals/Nalles Formation, NAL_2 - San Cosma e Damiano Member of the Nals/Nalles Formation, TGV - Tregiovo Formation, ORA_1 - Perdonig/Predonico Member of the Auer/Ora Formation, GAR - Gröden/Val Gardena Formation.

ty was mostly pyroclastic (ignimbrites) and composition switched from rhyodacites to rhyolites. Epiclastic products are generally subordinate to volcanic rocks and locally form interlayers at different levels of the succession that mark periods of less volcanic activity (Giannotti 1962; Cassinis & Neri 1992; Fels & Paul-Koch 1985; Barth & Mohr 1994; Aspmair & Krainer 1998; Krainer & Spötl 1998; Avanzini et al. 2007; Marocchi et al. 2008; Bargossi et al 2010). Located about halfway within the stratigraphic succession of the AG, the Guntschna/Guncina Formation is sandwiched between the Gargazon/Gargazzone and Nals/Nalles formations at the base and the Andrian/Andriano Formation on the top (Figs. 2, 3). The Guntschna/Guncina Formation represents one of the thickest and most continuous epiclastic successions in the AG. It is up to 250 m thick and crops out in a small area between the villages of Terlan/Terlano, Nals/Nalles and the city of Bozen/Bolzano (Figs. 1-3). The underlying Gargazon/Gargazzone Formation consists of a rhyodacitic ignimbrite up to 800 m thick formed by a giant caldera-forming eruption. After the development of a resurgent dome (Terlan/Terlano subvolcanic body), a collapse of the area south of Terlan/Terlano took place, with the formation of an evident morphological step (Avanzini et al. 2007; Morelli et al. 2012). The pyroclastic products of the Nals/Nalles Formation gradually filled the collapsed area. Later, the volcanic activity stopped, and the alluvial succession of the Guntschna/Guncina Formation was deposited throughout the area, filling and sealing the basin created by the collapse. The source of clastics was mainly represented by the northern areas affected by erosion of the volcanic products of the Gargazon/Gargazzone Formation. Finally, the alluvial and lacustrine deposits were covered by rhyolitic lava flows of the Andrian/Andriano Formation.

Materials and methods

The studied area is located in the northwestern part of the Athesian Volcanic District, between the capital of the Bozen/Bolzano Province and the city of Meran/Merano. The Bozen/Bolzano Province is historically bilingual (or trilingual in certain areas of the Dolomites), hence, each major city, locality and mountain has an equivalent name in German and Italian. Only very local toponyms were never translated and have only one name. Since villages have two names, also the lithostratigraphic formations named after these toponyms have two names. For a better understanding, in this paper both toponyms are used, separated by a "/", starting with the German name, since that is the historically older one. The two studied outcrops of Grissian/Grissiano (also called Grissian/Grissiano Gorge) and Gorl are located respectively on the orographic western (UTM (WGS84) coordinates: E: 667191; N: 5155402) and eastern slope (UTM (WGS84) coordinates: E: 673800; N: 5157424) of the Etsch/Adige Valley, at an approximate distance of 6.5 km from each other (Fig. 2).

Samples were collected from different lithologies within the Guntschna/Guncina Formation at both outcrops. Particularly, sandstones, siltstones, limestone beds and chert layers were sampled for the preparation of thin sections that were studied under a polarizing microscope. The sampling for palynological (palynofacies and quantitative sporomorphs study) and stable carbon isotope analyses was restricted to finer-grained, siliciclastic rocks, limestones and cherts of the Grissian/Grissiano and Gorl successions. The coarse-grained conglomerates were not sampled as they are barren regarding organic carbon and sporomorphs. The sampled interval of the Grissian/Grissiano section (31 metres) crops out mainly in sandy and silty facies, with intercalated dark grey siltstones/mudstones and limestone/chert layers; here, only 15 palynological and stable carbon isotope samples could be collected along the very steep outcrop (GR1-15, see Figs. 4, 9). The Gorl section is generally coarse-grained. For palynology and stable carbon isotope analyses 22 samples (GRL1-19, Figs. 6, 10) were collected from each intercalated fine-grained sandstones, siltstones and mudstones at distances of 25-30 cm. The sampled interval encompasses approximately 12 metres of the section.

These 37 palynological samples were described for their lithologies and colours (see Suppl. Tabs. 1 and 2). Afterwards, they were crushed to grains of several mm in size in order to increase sample surface area for acid digestion. The acid treatment was carried out by Rae Jones laboratory (UK) with 28% hydrochloric acid (HCl) and 60% hydrofluoric acid (HF) and treatment with additional HCl to dissolve fluorides formed by HF. The resultant residue was sieved at 10 μm, without ultrasonic. Permanent slides were produced by mounting the residue on cover slips with dilute polyvinyl alcohol as a dispersant, dried and subsequently mounted on a microscope slide with EPO-TEK® 301 epoxy resin. Slides are permanently stored at the Museum of Nature South Tyrol, Bozen/Bolzano.

The palynological slides were studied under a transmitted light microscope by counting 300 organic particles per slide for the palynofacies analyses. Three major categories of organic particles were distinguished following Tyson (1993, 1995): phytoclasts, palynomorphs (sporomorphs, fungal spores/hyphae), and amorphous organic matter (AOM). Phytoclasts were further subdivided into woody tissues, cuticles, thin membranes, charcoal, and opaque phytoclasts (equidimensional and lath-shaped, as well as those bigger and smaller than 50 μm). The term charcoal is used here for microscopic charcoal found in the palynological assemblages; no petrographic analyses have been carried out. Within the group of the sporomorphs, smooth and ornamented spores, monosaccate, bisaccate and asaccate pollen grains were distinguished. The state of preservation of woody tissues, cuticles, spores and pollen grains was noted as well (see Suppl. Fig. 1 and Suppl. Fig. 2).

For this study, several relative abundance ratios were calculated to elucidate stratigraphic trends (Tyson 1993, 1995) and as proxies for the distance of the depositional sites from the source of the sedimentary organic matter, as proposed by Tyson & Follows (2000). These include the ratio of small (<50 μm) to large (>50 μm) lath-shaped opaque phytoclasts; the equidimensional (equid.) to lath-shaped black opaque phytoclasts, and the well-preserved sporomorphs (wp) to degraded sporomorphs.

In addition to the palynofacies analysis, a quantitative sporomorph assemblage analysis was also carried out, with the counting of at least 300 sporomorphs in order to understand whether the observed changes in composition of the palynofacies are only related to a difference in transport and taphonomic selection, or if they can be attributed to external environmental and/or climate changes. The counted sporomorphs were assigned to their respective parent plants and subsequently to their ecoclimatic affinity (hygromorphic/xeromorphic) (Tab. 2) based on literature (Marchetti et al. 2022 and references therein).

The comparison between the samples of the Grissian/Grissiano and the Gorl sections was carried out based on the results of a principal component analysis (PCA) performed on a variance-covariance matrix with PAST statistical program (Hammer et al. 2001) using selected palynofacies categories. A Ternary plot created by R package: Ternary (Smith 2017) was employed to investigate the relations between the three major components of the PCA analyses to identify the different depositional environments.

For stable carbon isotope analyses, subsets of the palynological samples were powdered and treated with 10% hydrochloric acid overnight to remove all carbonates. The residues were then neutralized by washing with deionized water and dried at 40-60 °C in a ventilated oven. Between 5 and 20 mg of the treated powder were then weighted in tin vessels and analyzed with a Delta V Advantage isotopic ratio mass spectrometer, connected to a Thermo Flash 2000 Elemental Analyzer, at the Department of Geosciences, University of Padova. The obtained raw isotopic ratios were normalized with two international isotopic reference materials (CH-6 and CH-7) run along with the samples. All isotopic values are reported with respect to the VPDB scale. The analytical error was evaluated by running an internal quality control standard along with the samples (a sucrose from C_3 plants), and resulted to be better than ±0.15‰ (1 standard deviation) during the period of the analyses.

Facies analyses

At Grissian/Grissiano and Gorl, the sedimentary rocks of the Guntschna/Guncina Formation (FMG) are well exposed. The FMG is divided into a conglomeratic sandy facies (FMGa) and a sandy pelitic facies (FMGb) (Avanzini et al. 2007). The sedimentary succession is underlain by volcanic rocks of the Nals/Nalles Formation (NAL) at Grissian/Grissiano and by the Gargazon/Gargazzone Formation (IGG) and by "subvolcanic rocks" of the Terlan/Terlano Formation (TRL) at Gorl. At both sites, the sedimentary successions are overlain by rhyolithic volcanic rocks of the Andrian/Andriano Formation (LAN).

At Grissian/Grissiano the FMG is a >200 m thick fining-upward succession, starting with a coarse-grained conglomerate at the base that fines upward and grades into a sandstones-dominated facies, followed by fine-layered siltstones and sandstones, and finally into a limestones-cherts dominated facies on top (see Aspmair & Krainer 1998; Krainer & Spötl 1998; Hartkopf-Fröder et al. 2001). At Gorl, the FMG is only 100 m thick and mainly represented by sandy facies with some conglomerates at the base (Aspmair & Krainer 1998; Krainer & Spötl 1998; Hartkopf-Fröder et al. 2001).

Facies analysis of the Grissian/Grissiano section

The lithofacies types of the Grissian/Grissiano and Gorl sections are listed in Tab. 1.

At Grissian/Grissiano, the sedimentary succession starts with about 50 m of conglomerates lying on top of a very coarse pyroclastic breccia of the San Cosma e Damiano Member of the Nals/Nalles Formation (Fig. 4). The conglomerates are coarse-grained at the base, with clasts up to several dm in diameter, and grade into very coarse sandstones with lenses and layers of conglomerates with cm- to dm-large clasts.

The facies is massive, poorly sorted, and dominantly clast-supported (lithofacies Gcm-clast-supported massive gravel of Miall 1996, 2010), subordinately matrix-supported (lithofacies Gmm-matrix-supported massive gravel of Miall 1996, 2010). Upwards, approximately 80 m of thick-bedded sandstone beds follow. This succession is composed of mostly massive to horizontally laminated sandstones that are up to 3 m thick (lithofacies Sm-sandstones with massive or faint lamination and Sh-sandstones with horizontal lamination according to Miall (1996, 2010) with rare intercalations of conglomerates dispersed in a sandy matrix.

The conglomeratic succession passes upward gradually to a sandy and silty interval. This facies is about 35 m thick, well stratified with 5 to 30 cm thick layers and is characterized by massive to horizontally laminated sandstone beds (lithofacies Sm and Sh of Miall 1996, 2010) alternating with thin, dark grey siltstone and mudstone beds that are commonly a few cm thick. Rare intercalations of cross-bedded sandstone beds up to 1 m thick (lithofacies St-sandstones with trough crossbedding of Miall 1996, 2010) and fine conglomerates are present too. Photos of the sandy and silty lithofacies of the Grissian/Grissiano section are shown in Fig. 5.

Main lithofacies types		
Fluvial lithofacies types		
Code	**Description**	**Interpretation**
Gcm	clast-supported massive gravel	pseudoplastic debris flow
Gmm	matrix-supported massive gravel	plastic debris flow
Sm	sandstones, massive	sheetflood, flashflood deposits
Sh	sandstones, horizontal laminations	sheetflood, flashflood deposits
Sr	sandstones, ripple cross lamination	current ripples
St	sandstones, trough crossbedding	channel fill deposits
Fl	siltstones, mudstones, laminated	waning flood deposits
Lacustrine lithofacies types		
Fsm	fine-grained sandstones, siltstones, mudstones, laminated	fine-grained lacustrine deposits
Lsl	limestones, laminated	lacustrine microbial mats (stromatolite)
Lm	micritic limestones	lacustrine limestones, cyanobacteria
Ch	chert layers and beds	lacustrine abiogenic precipitations
Onc	oncolite beds	lacustrine, freshwater oncoids
Cac	caliche crust	pedogenic limestones

Tab. 1 - Main fluvial and lacustrine lithofacies types. Codes of the fluvial facies after Miall (1996, 2010).

The overlaying limestone-dominated facies is about 7-8 m thick (Fig. 4). The most abundant lithologies are laminated beds composed of limestones (Lsl). These laminated beds are up to about 20 cm thick and interbedded with dark grey laminated silt- and mudstones (Fsm). A carbonate breccia bed occurs in the middle of this facies, it is up to 4 m thick and composed of dm-sized clasts, embedded in a fine-grained matrix. According to Krainer & Spötl (1998), the laminated limestone beds are composed of alternating thin layers of (calcimicrobial) laminites, dark micritic limestones (Lm), cherts (Ch), siltstones-mudstones (Fsm) and rare thin caliche crusts (Cac). Limestones are mostly recrystallized, rare laminated limestone layers display structures indicating that they are formed by freshwater cyanobacteria or other calcimicrobes.

Chert layers are translucent to transparent and commonly contain brown organic fragments and well-preserved sporomorphs. Locally, abundant well-preserved pollen grains are embedded in the chert layers. The most abundant petrographic type of chert is microflamboyant quartz, locally microcrystalline chert and megaquartz are present. Subordinately, chalcedony occurs as well (for details see Krainer & Spötl 1998).

Facies analysis of the Gorl section

At Gorl (Figs. 6, 7), the sedimentary succession of the Guntschna/Guncina Formation starts with breccias and conglomerates that are poorly exposed along the road to Gorl with a thickness of approximately 30 m ("conglomeratic facies"). They directly overlie rhyodacitic ignimbrites of the Gargazon/

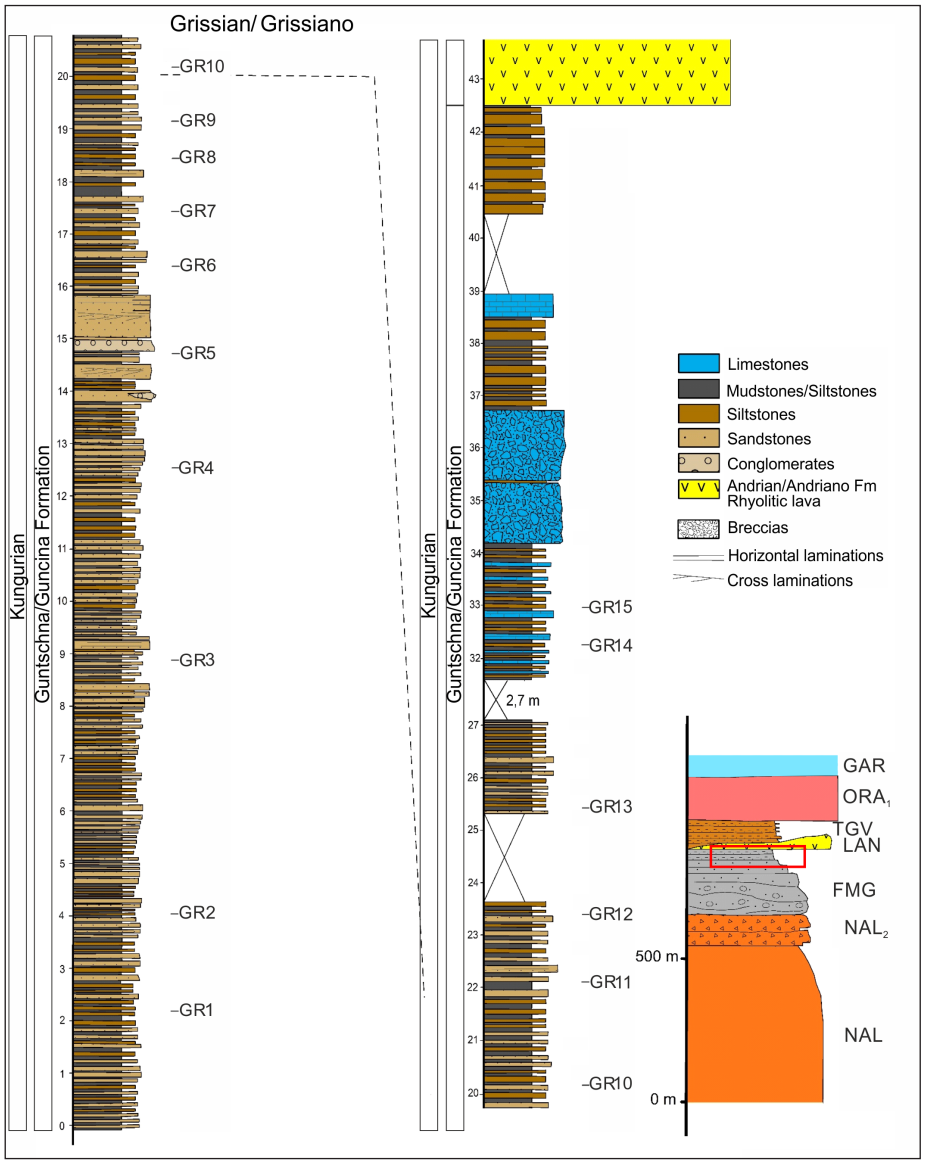

Fig. 4 - Detailed stratigraphic log of the upper part of the Grissian/Grissiano section and its position within the Guntschna/Guncina Formation (FMG). The position of the samples collected for palynological/stable carbon isotope analyses is indicated. For key of colours and abbreviations in the overall section see Fig. 2. Photos of the main lithofacies of the Grissian/Grissiano section are presented in Fig. 5.

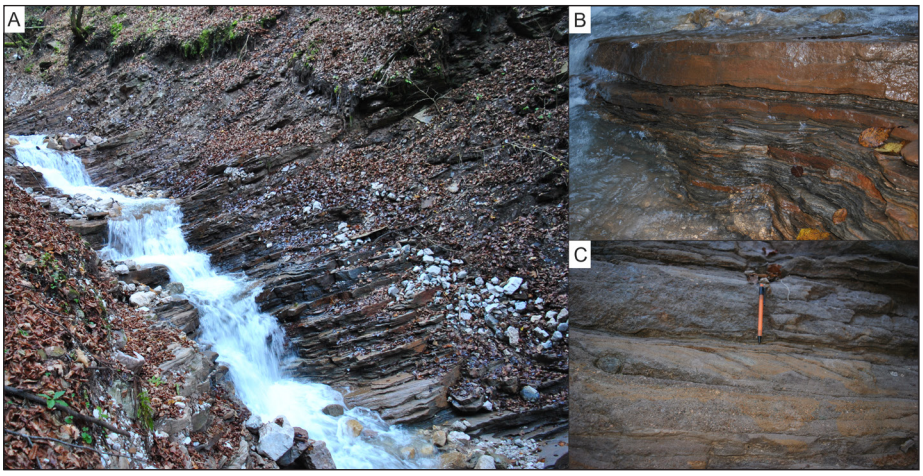

Fig. 5 - Examples of lithofacies types from the Grissian/Grissiano section. A) Outcrop of the sandy and silty interval along the Grissian/Grissiano creek; B) Siltstone and mudstone beds alternating with massive to horizontally laminated sandstone beds; C) Horizontally laminated and cross-bedded sandstone beds.

Gargazzone Formation. This coarse-grained succession is poorly sorted and composed of different types of volcanic clasts that are angular to well-rounded and contain sandy matrix (lithofacies Gcm of Miall 1996, 2010; Tab. 1). Grain-size is mostly < 10 cm; individual clasts are up to 1 m in diameter.

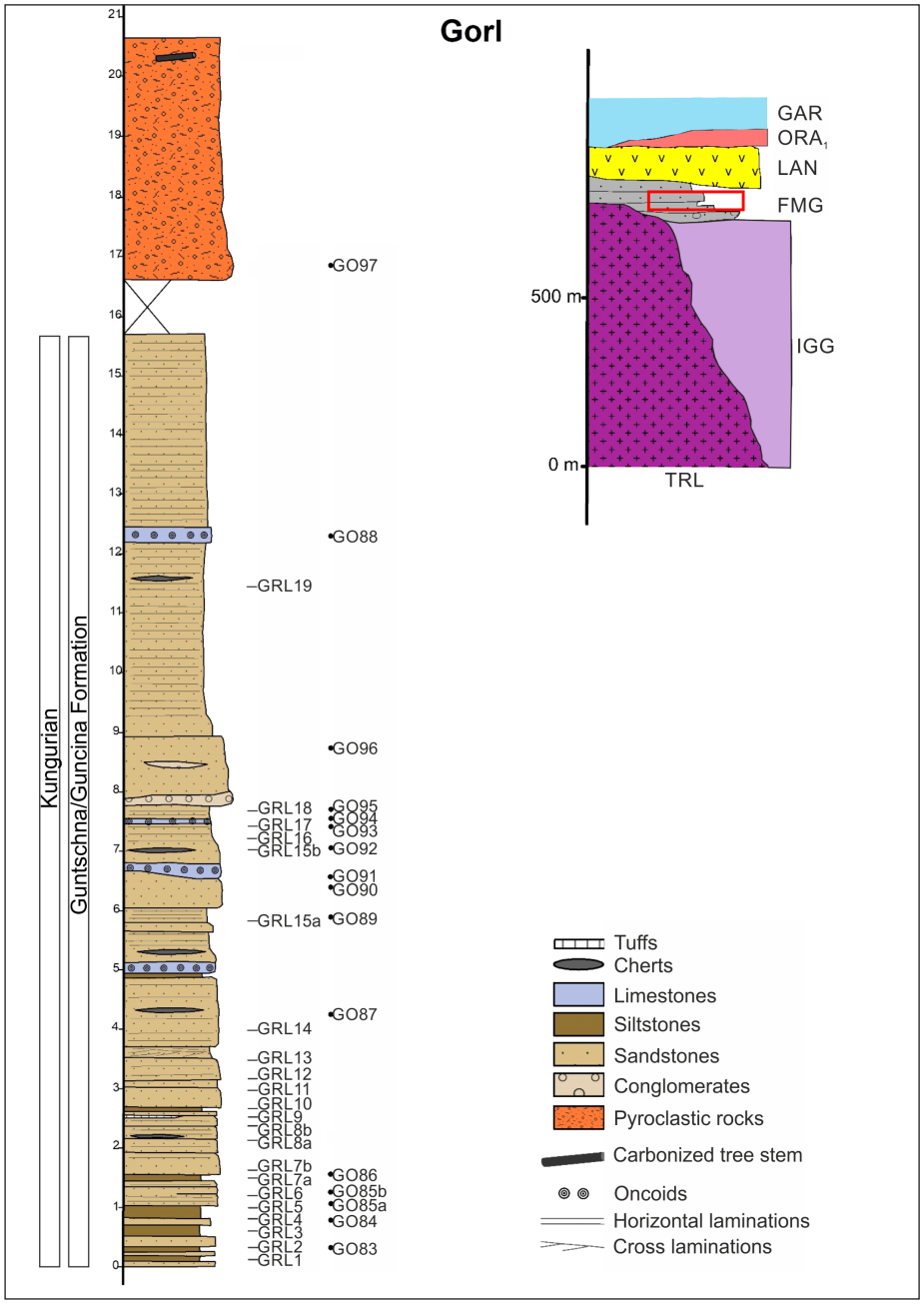

Fig. 6 - Detailed stratigraphic log of the studied part of the Gorl section and its position within the Guntschna/Guncina Formation (FMG). The position of the samples collected for palynological/stable carbon isotope analyses (GRL) and those for facies analyses (GO) is indicated. For key of colours and abbreviations in the overall section see Fig. 2. Photos of the main lithofacies of the Gorl section are presented in Fig. 7.

The conglomeratic facies is followed by a covered interval of 20-30 m, and then by an exposed sedimentary succession that is approximately 20 m thick and composed of the following lithotypes (see also Aspmair & Krainer 1998; Krainer & Spötl 1998; Hartkopf-Fröder et al. 2001) (Tab. 1; Figs. 6-8):

Fine- to coarse-grained, mostly massive to indistinctly horizontally laminated beds of sandstones up to 3-4 m thick are the dominant lithofacies (lithofacies Sm and Sh of Miall 1996, 2010; see Fig. 7). Less abundant are horizontally laminated, fine-grained sandstones (Sh), commonly interbedded with thin siltstones; thickness is <50 cm, mostly < 30 cm. Many of the fine-grained sandstone units contain abundant small plant debris. Cross-bedded sandstones are rare and occur in 20 to 60 cm thick units (lithofacies St of Miall 1996, 2010). Pebbly sandstones with clasts up to 5 cm in diameter are present in the middle part of the section. A few sandstone units display synsedimentary deformation structures.

Siltstones to muddy siltstones occur as thin (mostly < 10 cm) intercalations in fine-grained sandstones (lithofacies Fl of Miall 1996, 2010). Many siltstone beds contain abundant small plant fragments, rarely ostracods (Fig. 8C, 8E). Nodular siltstone beds up to 25 cm are present and composed of calcite-cemented, partly silicified siltstones.

Fig. 7 - Examples of the lithofacies types from the Gorl section. A) Outcrop of the sandstones dominated succession overlain by lava flows of the Andrian/Andriano Formation (cliff on the top); B) Massive to horizontally laminated amalgamated sandstone beds; C) Fine-grained sandstones interlayered with siltstones and muddy siltstones.

Carbonate and chert layers are up to 60 cm, mostly a few cm to 30 cm thick, laminated and commonly made of alternating thin carbonate (often microbialites, Lsl) and chert layers (Ch) and lenses (Fig. 8A, 8B), the latter containing well preserved sporomorphs (Fig. 8A). Individual laminae are up to a few mm thick. Carbonate layers are recrystallized, rarely showing structures indicating the presence of cyanobacteria (Fig. 8D).

Thin siltstones to fine-grained sandstone layers (Fsm) are also intercalated with carbonate and chert layers. Individual carbonate and chert layers are irregular and often lense out laterally.

Oncolite layers (Onc) are up to 30 cm, mostly 5-20 cm thick and contain oncoids up to approximately 2 cm in diameter. Oncoids are composed of nuclei that are mostly formed of micritic grains, less commonly of ostracod shells and siliciclastic grains such as volcanic quartz grains and volcanic rock fragments. The nuclei are surrounded by laminae that display radial structures. All oncoids are recrystallized. Oncoids are partly fragmented. Rarely, thin (1 mm) microbial layers are intercalated. Individual oncolite beds contain micritic and pelmicritic carbonate grains. The matrix is a mixture of micrite and siliciclastic material.

The exposed succession is covered by a pyroclastic layer of about 4-5 m thickness that contains in the upper part fragments of coalified stems. The sedimentary succession of the Guntschna/Guncina Formation above the pyroclastic rock is about 30 m thick but poorly exposed in scattered outcrops. It is overlain by a more than 100 m thick horizon of rhyolitic lavas belonging to the Andrian/Andriano Formation (see Fig. 7).

Palynofacies analyses

Palynofacies analyses of the Grissian/Grissiano section

The palynofacies assemblages of the Grissian/Grissiano section are composed of terrestrial particles; black opaque phytoclasts and palynomorphs (Figs. 9, 11: A-D; Suppl. Fig. 1). The opaque phytoclasts reach up to 94 % (in GR13) with the small opaque phytoclasts (≤ 50 μm) being the dominant subcategory, reaching up to 53 % of the total particles. The sporomorphs (1.5-49 %) are mainly composed of bisaccate, monosaccate and asaccate pollen grains. Spores are rare (<2 %). Woody tissues and cuticles are also occasionally abundant (1.8-48 %)

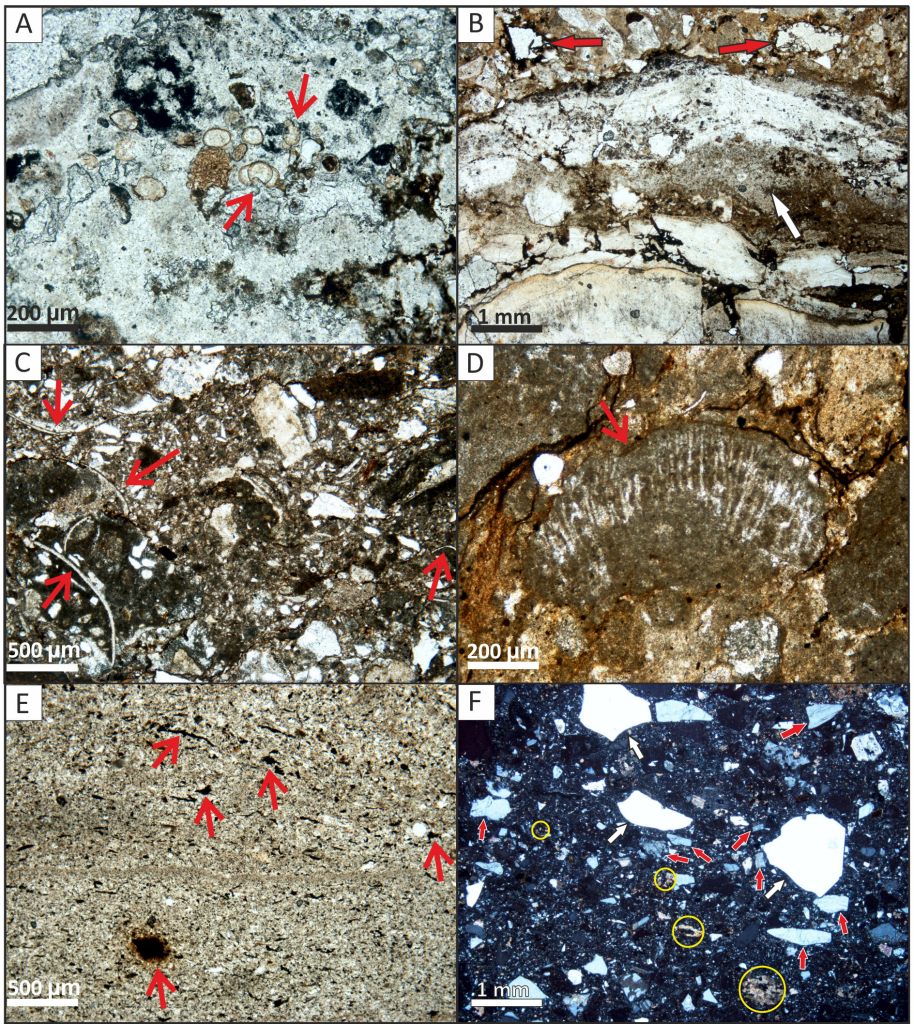

Fig. 8 - Examples of common microfacies types from the Gorl section as seen with non-polarized light (A-E) and polarized light (F). A) Thin chert layer containing well-preserved bisaccates pollen grains (centre, red arrows). Sample GO 86; B) Thin irregular chert layers (one indicated with white arrow) alternating with layers containing sand-sized grains, mainly volcanic quartz (red arrows). Sample GO 87-3; C) Indistinctly laminated sediment composed of silty matrix with micritic grains, few quartz grains and ostracod shells (red arrows). Sample GO 88d-2; D) Cyanobacteria (probably *Rivularia*, red arrow) in a carbonate bed. Sample GO 88b; E) Siltstones, indistinctly laminated, containing abundant small organic (plant) debris (some indicated by red arrows). Sample GO 89-1; F) Sandstone composed of monocrystalline quartz (thick white arrows), feldspars (thick red arrows), volcanic cherts and few volcanic rock fragments (yellow circles). Detrital grains are cemented by calcite. Sample GO 90.

and mostly degraded (Fig. 9 and Suppl. Fig. 1). The AOM is a rare to common component (0-6 %). Charcoal fragments are almost completely absent in the lower part of the succession while in the upper part, from GR7 onwards, they are becoming more abundant (0.3-5.5%). The sporomorphs (mostly bisaccate pollen grains, see Suppl. Fig. 1) are generally well preserved (Fig. 9; Suppl. Fig. 1). Their abundance in the palynofacies fluctuates together with the non-opaque phytoclasts (woody tissues and cuticles), relatively opposing to the black opaque phytoclasts. In GR7, at approximately 17 m (Fig. 9) from the base of the studied succession, the palynomorphs increase rapidly in abundance, reaching ~49 %, and keep relatively high values up to 24 m from the section base. Charcoal fragments show two relative peaks in abundance, respectively 17 and 21 m above the base of the sampled succession. The ratio small lath-shaped opaque phytoclasts (OP l.s. small) to large lath-shaped opaque phytoclasts (OP l.s. large) varies from 0 to 0.7 and shows relatively higher values starting from 14 m upwards in the section. The ratio equidimensional to lath-shaped opaque phytoclasts (Fig. 9) varies from 0.52 to 0.86 but decreases linearly, in the upper part of the section, starting with sample GR7. The generally good preservation of sporomorphs is indicated by the well-preserved (wp) to non-well-preserved ratio, especially between 12 and 24 m, whereas in samples GR3, GR13, GR14, and GR15 the preservation is moderate.

Palynofacies analyses of the Gorl section

The palynofacies assemblages in the Gorl section is composed of terrestrial organic particles. The major components of the Gorl palynofacies throughout the section are opaque black phytoclasts (~83 %), especially those < 50 µm (Figs. 10, 11: E-H; Suppl. Fig. 2). Common to scarcely present (0-14 %) are the woody tissues and cuticles (non-opaque phytoclasts) with different states of preservation, whereas charcoal is rare (<1 %). Sporomorphs are mostly bisaccate pollen grains (Suppl. Fig. 2) and trilete spores (Figs. 10, 11) that are

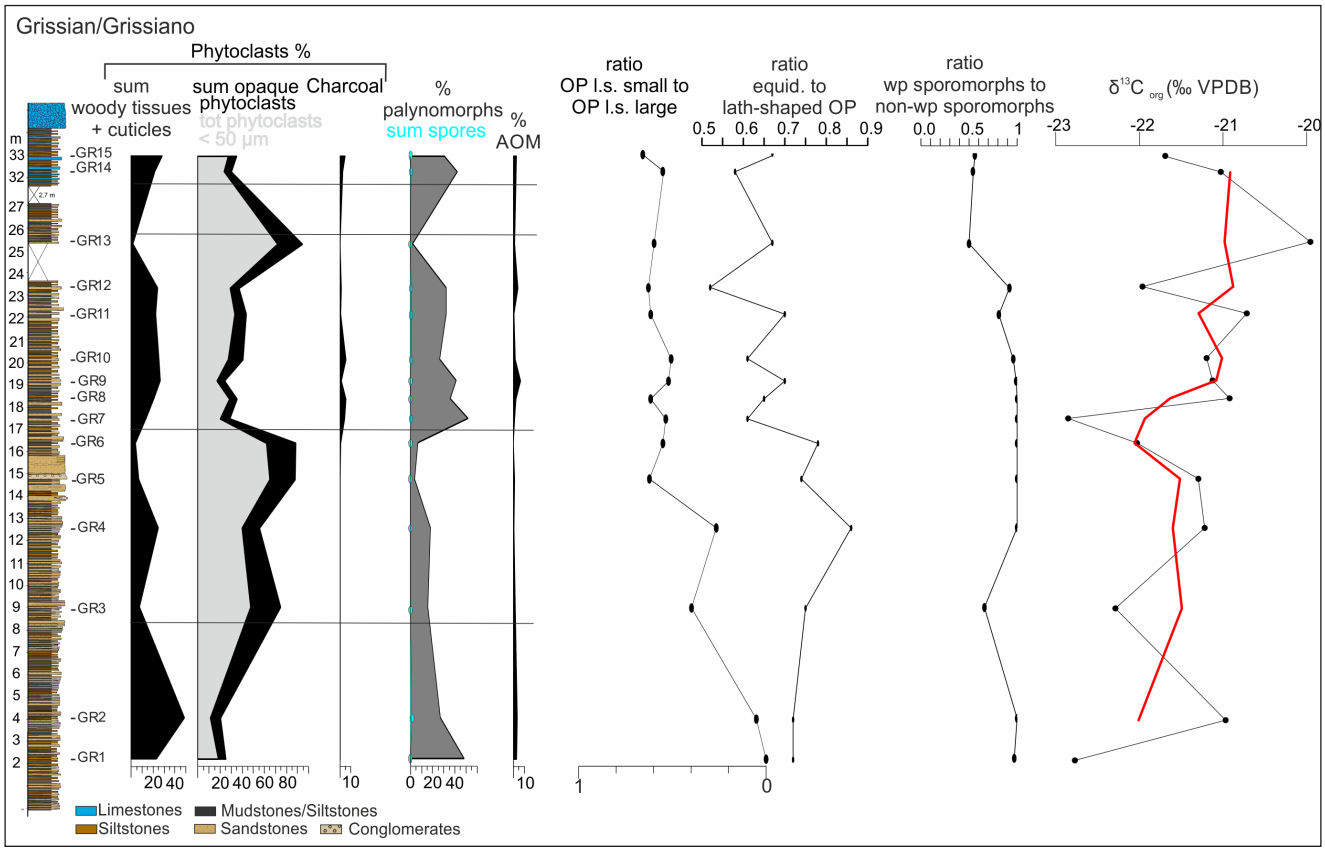

Fig. 9 - Stratigraphic column of the Grissian/Grissiano section and position of the palynological/stable carbon isotope samples. The palynofacies diagram shows the major components expressed in percentages. Additionally, the ratio between the lath-shaped opaque phytoclasts < 50 µm (= OP l.s. small) and the lath-shaped opaque phytoclasts > 50 µm (= OP l.s. large), the equid. (= equidimensional) to lath-shaped opaque phytoclasts ratio, the ratio between well-preserved (wp) to not well-preserved sporomorphs, and the $\delta^{13}C_{org}$ are provided. Red line in $\delta^{13}C_{org}$ column is the 3-points moving average.

generally moderately preserved in the lower part of the section (GRL1-3). Their relative abundances fluctuate noticeably (1-47 %) within the first ca. 4 m from the base of the section, and are almost absent in samples GRL15b to GRL17, where opaque phytoclasts are dominant. The AOM is generally rare (< 2%) throughout the section but is almost absent in the middle part of the succession. The ratio small lath-shaped opaque phytoclasts (OP l.s. small) to large lath-shaped opaque phytoclasts (OP l.s. large) shows higher values after the first three samples (from the bottom of the section) and relatively higher fluctuations between 2-4 m; within the remaining section variations are relatively smaller (Fig. 10). The ratio between equidimensional to lath-shaped opaque phytoclasts fluctuates noticeably from 0.59 to 0.84 between 0-4 m of the section (GRL1-14), but gets more stable in the middle and upper part of the section. The ratio well-preserved to non-well preserved sporomorphs indicates a poor preservation throughout the section, especially between 7 and 7.5 m (GRL15b, GRL16, GRL17), while a moderate preservation has been observed between 2.5 and 6 m.

Quantitative sporomorph analysis of Grissian/Grissiano and Gorl sections

In addition to palynofacies analyses, sporomorphs were identified at genus level and assigned to their parent plants and ecoclimatic affinity (xeromorphic, xeromorphic-hygromorphic, hygromorphic, see Tab. 2). Most abundant sporomorphs are shown in Suppl. Fig. 3. In the Grissian/Grissiano samples it was possible to count 300 sporomorphs per sample. Three samples from the Gorl section (GRL15b, GRL16, GRL17) in which the opaque phytoclasts reach almost 100 %, are barren with regard to sporomorphs whereas sample GRL13 has a poor pollen content.

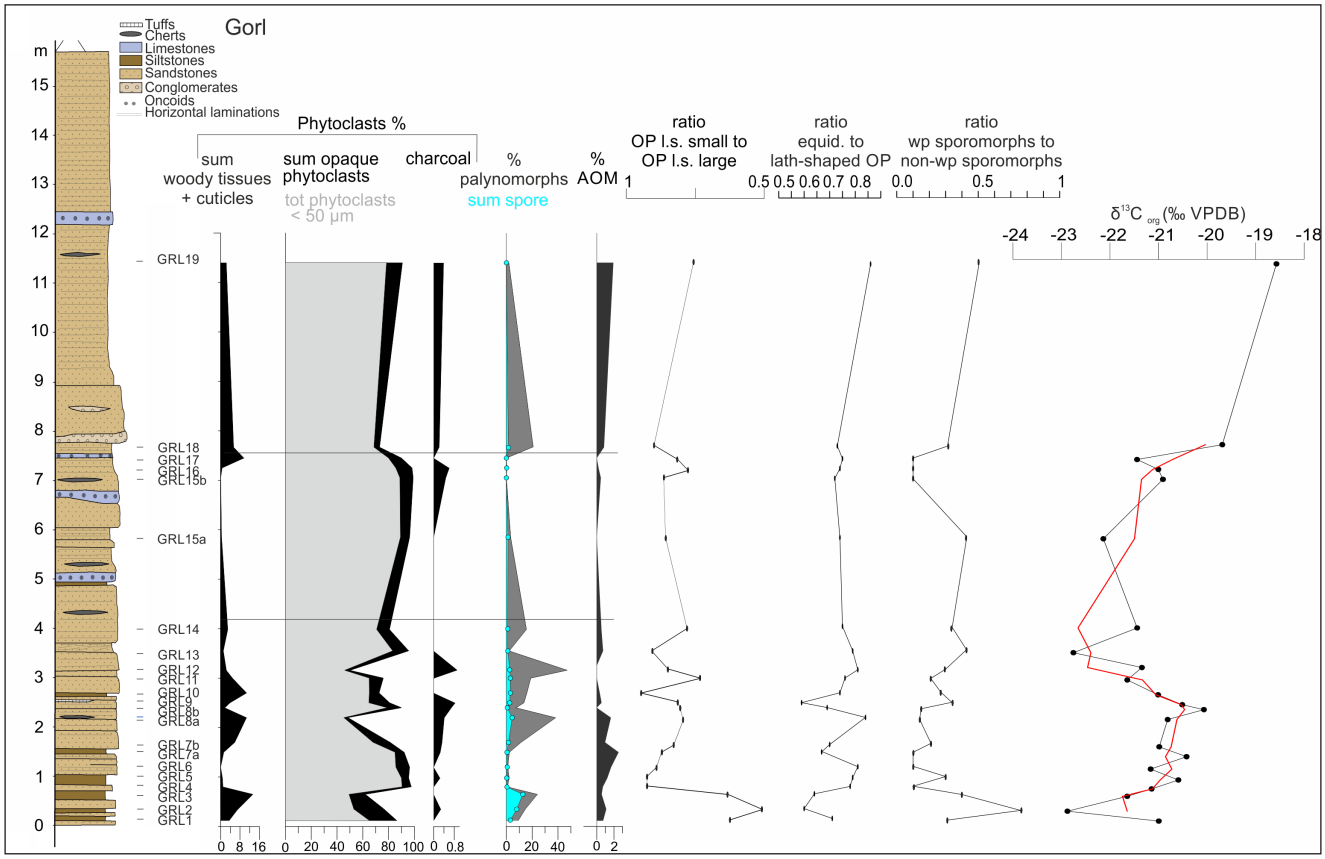

Fig. 10 - Stratigraphic column of the Gorl section with position of the palynological/stable carbon isotope samples. The palynofacies diagram shows the major components expressed in percentages. Additionally, the ratio between the lath-shaped opaque phytoclasts < 50 µm (= OP l.s. small) and the lath-shaped opaque phytoclasts > 50 µm (= OP l.s. large), the equid. (= equidimensional) to lath-shaped opaque phytoclasts ratio, the ratio between well-preserved (wp) and not well-preserved sporomorphs, and the $\delta^{13}C_{org}$ values are provided. Red line in $\delta^{13}C_{org}$ column is the 3-points moving average.

The sporomorph assemblages of Grissian/Grissiano and Gorl sections are composed of the same taxa. Twenty-five pollen and seven spore genera and species were encountered. The abundances of the taxa from the Grissian/Grissiano section are shown in Fig. 12, and for the Gorl section in Fig. 13. With the exclusion of indeterminable bisaccate pollen grains (Bisaccate indet., Tab. 2, Figs. 12, 13), the line charts in Figs. 14 and 15 summarize the changes of the three ecoclimatic groups throughout the two studied sections.

The ecoclimatic diagram of the Grissian/Grissiano section (Fig. 14) does not show pronounced fluctuations. The intermediate taxa (xeromorphic-hygromorphic), mainly corresponding to Peltaspermales, Corystospermales and undifferentiated seed ferns (Tab. 2), dominate the assemblages (50-85 %) and co-variate with the xeromorphic taxa, mostly derived from conifers (Voltziales, Ullmanniaceae and Utrechtiaceae). Between ~17 and ~24 m from the base of the studied succession, there is an increase of the xeromorphic components and a corresponding decrease of the intermediate taxa, whose line displays a general increase towards the upper part of the section. The hygromorphic elements show a slight increase (see the smoothed values given by 3-points moving average in Fig. 14) around 16.5 m from the base of the studied section.

The ecoclimatic diagram of the Gorl section (Fig. 15) shows relatively larger variations within the first 3.5 m of the studied succession (GRL1-GRL13). Within the first 0.5 m, the hygromorphic taxa dominate the Gorl assemblages. These are spores from lycophytes and ferns (Tab. 2), plants flourishing in a wet habitat probably near the waterbody and accordingly closer to the depositional site than the xeromorphic-hygromorphic and xeromorphic vegetation. From 0.5 m up to ~2.7 m, the intermediate taxa dominate the assemblages. From GRL13 at 3.5 m upwards, intermediate taxa decrease corresponding to a single peak of hygromorphic taxa and a general increase of xeromorphic elements.

Taxa	**Pollen/ spore**	**Botanical affinity**	**Reference**	**Ecoclimatic affinity**
Bisaccate indet.	pollen	undefined		Not attributed
cf. *Cirratriradites*	spore	lycophytes, Selaginellales		hygromorphic
cf. *Florinites*	pollen	Cordaitales		hygromorphic
cf. *Granulatisporites*	spore	ferns, Botryopteridales, Lyginopteridales	Potonié 1962; Balme 1995; Looy & Hotton 2014	hygromorphic
cf. *Lycopodiacites*	spore	lycophytes, Lycopodiales		hygromorphic
Kraeuselisporites	spore	lycophytes, Lycopodiales, Selaginellales	Kustatscher et al. 2010; Raine et al. 2011	hygromorphic
cf. *Lophotriletes*	spore	lycophyte or fern		hygromorphic
Thymospora	spore	ferns, Marattiales	Looy & Hotton 2014	hygromorphic
Trilete psilate spores	spore	lycophyte or fern		hygromorphic
Verrucosisporites	spore	ferns, Marattiales, *in situ* in *Eoangiopteris goodii*; sphenophytes, Equisetales, *in situ* in *Bromsgrovia willsii*; seed ferns, Zygopteridales, *in situ* in *Corynepteris*	Taylor et al. 2009; Seyfullah et al. 2013	hygromorphic
Gardenasporites	pollen	conifers, Ullmaniaceae		xeromorphic
Gigantosporites	pollen	conifers, Ullmaniaceae	Clement-Westerhof 1974	xeromorphic
Illinites/Jugasporites	pollen	conifers, Voltziales, *in situ* in *Willsiostrobus*	Grauvogel-Stamm 1978; Kustatscher et al. 2010; Looy & Hotton 2014	xeromorphic
Limitisporites	pollen	conifers, Ullmanniaceae	Balme, 1995	xeromorphic
cf. *Limitisporites*	pollen	conifers		xeromorphic
Lueckisporites	pollen	conifers, Ullmanniaceae, *in situ* in *Majonica alpina* Clement-Westerhof 1987, but associated also with other conifers	Clement-Westerhof 1974, 1987; Meyen 1997	xeromorphic
Monosaccate degraded	pollen	conifers indet.		xeromorphic
Nuskoisporites	pollen	conifers, Voltziales, *in situ* in *Ortiseia* Florin 1964; Utrechtiaceae	Clement-Westerhof 1987; Balme 1995; Poort et al.1997; Looy & Hotton 2014	xeromorphic
Perisaccus	pollen	conifers indet.		xeromorphic
Potonieisporites	pollen	Voltziales, Ullmanniaceae; *in situ* in *Otovicia hypnoides*; Rufloriaceae, Emporiaceae, Utrechtiaceae	Balme 1995; Hernández-Castillo et al. 2001; Rothwell et al. 2005	xeromorphic
Trizonaesporites grandis	pollen	conifers, Voltziales, *in situ* in *Ortiseia* Florin 1964; Utrechtiaceae	Clement-Westerhof 1987; Balme 1995; Poort et al.1997; Looy & Hotton 2014	xeromorphic
Alisporites	pollen	seed ferns, Corystospermales (*Pteruchus*), Peltaspermales (e.g., *Amphorispermum, Autunia conferta*); conifers, Voltziales, Ullmanniaceae (*Ullmannia*), Voltziales (*Willsiostrobus*)	Balme 1995	xeromorphic-hygromorphic-
cf. *Costapollenites*	pollen	uncertain		xeromorphic - hygromorphic
Ephedripites	pollen	Ginkgophyta or seed ferns, Peltaspermales		xeromorphic-hygromorphic
Falcisporites	pollen	seed ferns, Corystospermales (*Pteruchus*), Peltaspermales (e.g., *Amphorispermum, Autunia conferta*); conifers, Voltziales, Ullmanniaceae (*Ullmannia*), Voltziales (*Willsiostrobus*)	Balme 1995	xeromorphic-hygromorphic
Klausipollenites	pollen	seed ferns, Peltaspermales or conifers	Raine et al. 2011; Mishra et al. 2017	xeromorphic-hygromorphic
Paravesicaspora	pollen	seed ferns, ?Callistophytacea, ?Peltaspermaceae	Looy & Hotton 2014	xeromorphic-hygromorphic
Platysaccus	pollen	seed ferns, Peltaspermales	Mishra et al. 2017	xeromorphic-hygromorphic
Striatites	pollen	seed ferns indet.		xeromorphic-hygromorphic
Striatopodocarpites	pollen	seed ferns indet.		xeromorphic-hygromorphic
Strotersporites	pollen	seed ferns indet.		xeromorphic-hygromorphic
Taeniaesporites	pollen	seed ferns, Corystospermales	Traverse 2007	xeromorphic-hygromorphic
Vesicaspora schemeli	pollen	seed ferns, Callistophytales, *in situ* in *Callospermarion, Idanothekion*; Peltaspermales	Kerp 1988; Balme 1995; Zavialova & van Konijnenburg-van Cittert 2011; Looy & Hotton 2014	xeromorphic-hygromorphic
Vestigisporites	pollen	seed ferns		xeromorphic-hygromorphic
Vittatina	pollen	seed ferns, Peltaspermales	Balme 1995; Looy & Hotton 2014	xeromorphic-hygromorphic

Tab. 2 - Sporomorph taxa identified in Grissian/Grissiano and Gorl sections with their botanical and ecoclimatic affinities (xeromorphic, xeromorphic-hygromorphic and hygromorphic taxa).

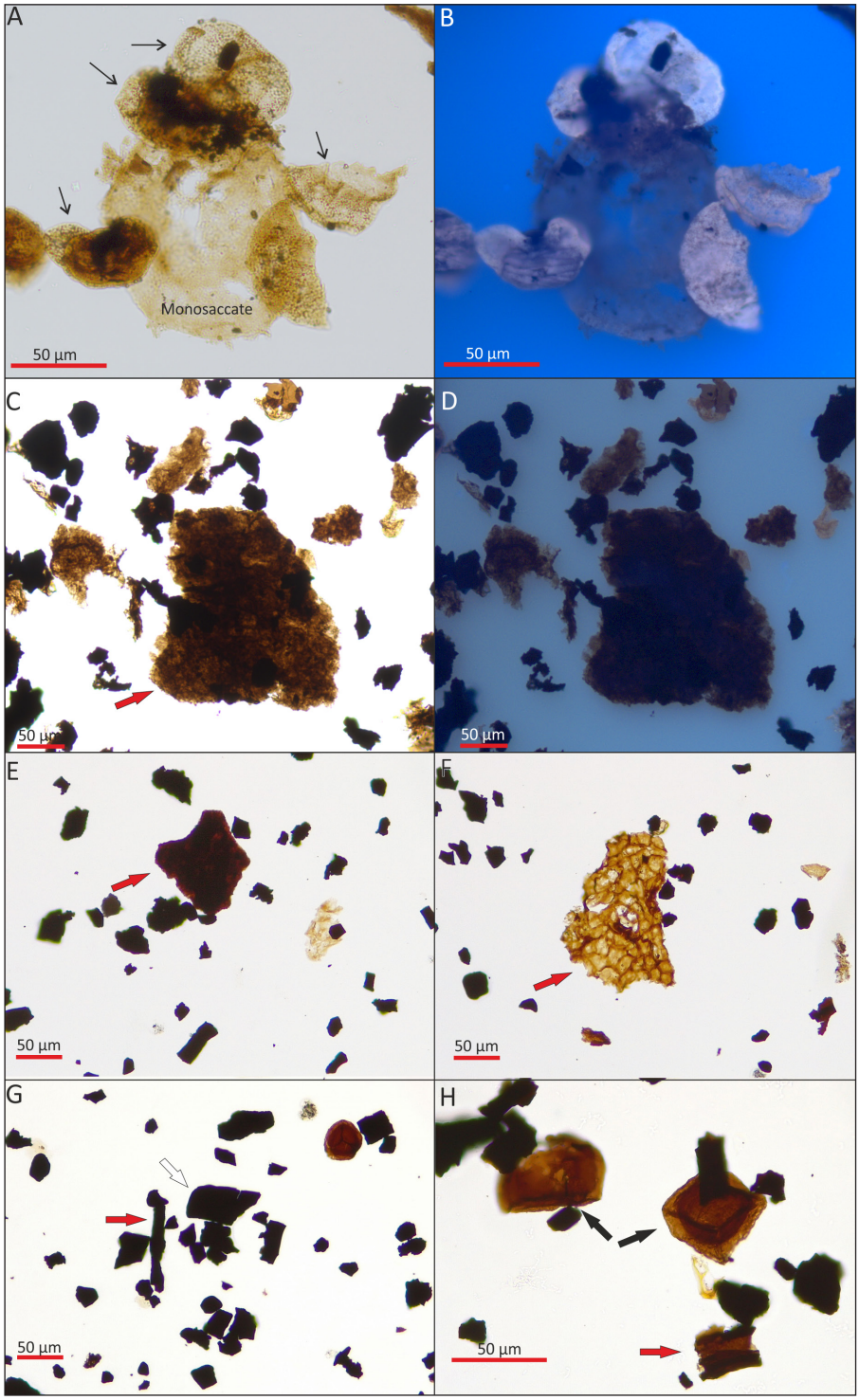

Fig. 11 - Examples of the palynofacies from the Grissian/Grissiano (A-D) and the Gorl (E-H) sections. Photographs were taken under transmitted light (A, C, E-H) and with ultraviolet fluorescent light (B, D). EF = England Finder. A) Five pollen grains showing different degrees of preservation: a mostly degraded large monosaccate and four smaller bisaccate pollen grains/fragments. Sample GR7, EF: N55-1. B) Same view as in A. The difference in fluorescence intensity between the sacci indicates the varying degree of preservation. The less degraded bisaccates display a more intensive fluorescence; the degraded monosaccate almost shows no fluorescence. C) Different types of phytoclasts. Red arrow: degraded woody tissue. Sample GR2, EF: J67. D) Same view as in C. The woody tissues and the black opaque phytoclasts do not show fluorescence. E) Small (<50 µm) black opaque phytoclasts equidimensional and lath-shaped together with a degraded woody particle (indicated with the red arrow). Sample GRL5, EF: H53-2. F) Small black opaque phytoclasts and a slightly degraded cuticle (indicated by the red arrow). Sample GRL3, EF: H38. G) Large (> 50 µm) lath-shaped black opaque phytoclasts (indicated by the red arrow) and large (>50 µm) equidimensional opaque phytoclast (indicated by the white arrow) and small (<50 µm) equidimensional opaque phytoclasts. A trilete spore is also visible at the upper right corner. Sample GRL2, EF: O52. H) Two trilete spores (indicated by the black arrows) and a well-preserved woody particle (indicated by the red arrow). Black equidimensional opaque phytoclasts are also present. Sample GRL1, EF: O44-2.

Stable carbon isotopes

The $\delta^{13}C$ of organic matter ($\delta^{13}C_{org}$) in bulk rock samples of the Grissian/Grissiano section varies between -22.8 ‰ and -20 ‰ (Figs. 9, 14). No clear trends were observed along the investigated succession. The $\delta^{13}C_{org}$ in bulk rock samples of the Gorl section varies within ca. -22.9 ‰ and -18.6 ‰ (Figs. 10, 15), i.e., similar to that of the Grissian/Grissiano section but with some exceptionally heavy samples. Even the heavier values, however, are not unusual for Permian organic matter or fossil plants. Lighter isotopic values of less than -21 ‰ seem to cluster in the middle of the section, but given that only a short interval of about 12 m could be investigated, we refrain from interpreting these data of the isotopic record as a significant feature.

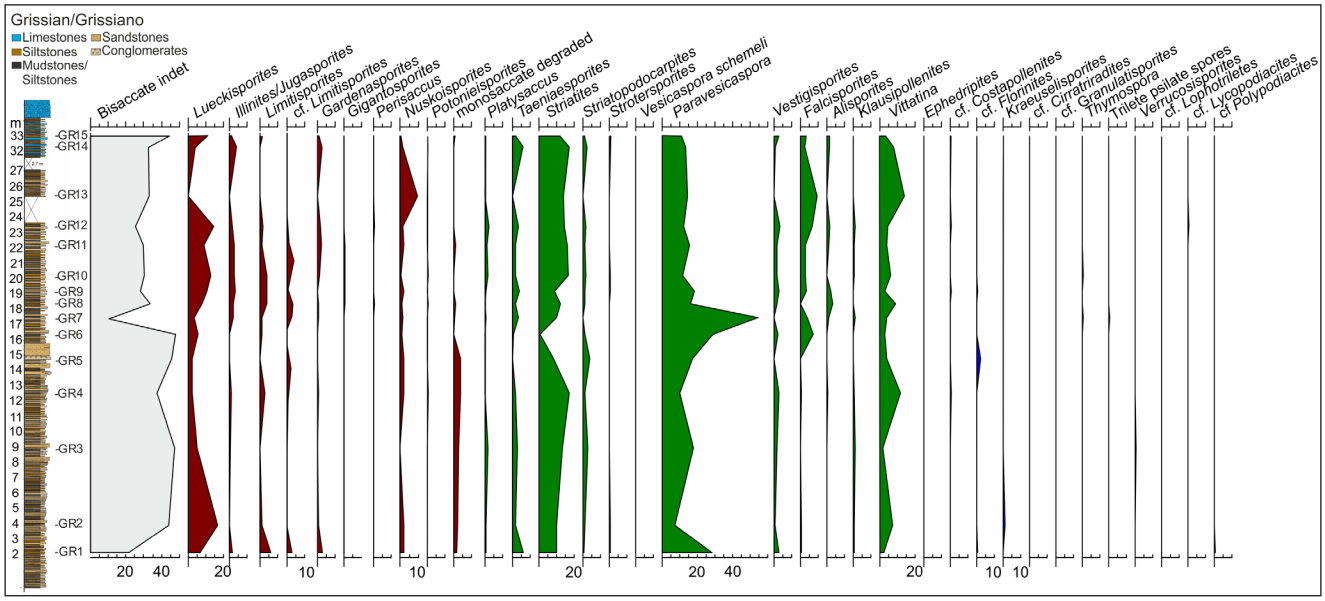

Fig. 12 - Relative percentage curves of the pollen and spore taxa identified in the Grissian/Grissiano section. The dark red filling indicates the xeromorphic taxa, the green filling the xeromorphic-hygromorphic taxa (intermediate), the blue filling indicates the hygromorphic taxa. Bisaccate indet. cannot be classified in the three ecoclimatic categories, therefore this group is excluded from the cumulative diagram shown in Fig. 14.

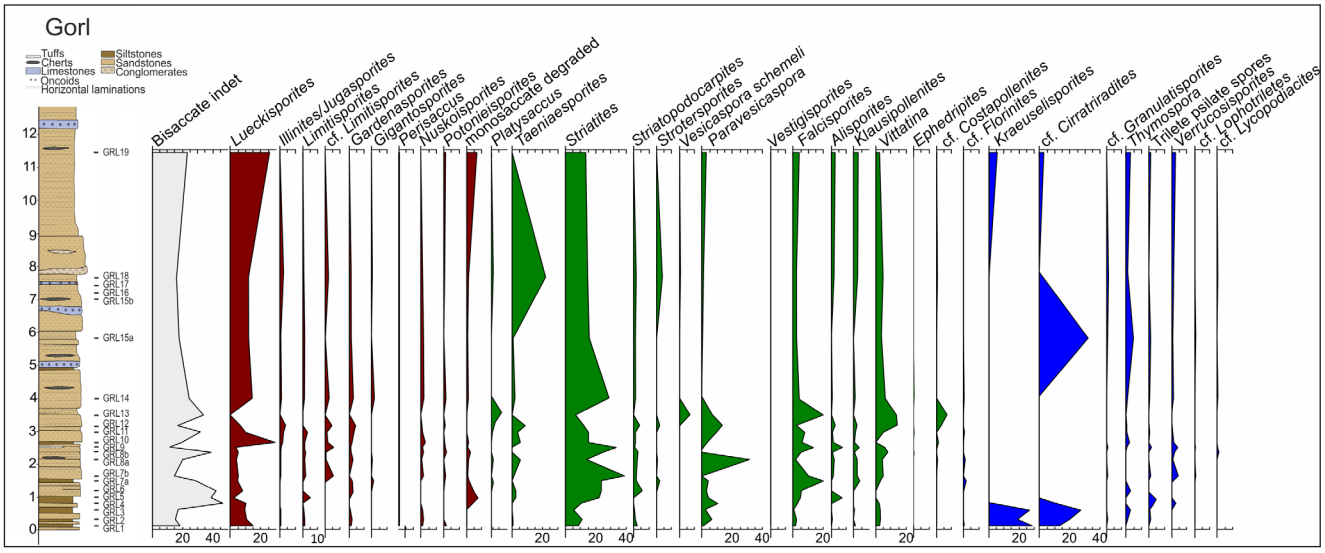

Fig. 13 - Relative percentage curves of the pollen and spore taxa identified in the Gorl section. The dark red filling indicates the xeromorphic taxa, the green filling the xeromorphic-hygromorphic taxa (intermediate), the blue filling indicates the hygromorphic taxa. In samples GRL15b, 16, 17 sporomorphs are very rare and are not shown in this diagram. Bisaccate indet. cannot be classified in the three ecoclimatic categories, therefore this group is excluded from the cumulative diagram shown in Fig. 15.

Discussion

The sections of Grissian/Grissiano and Gorl are located at an aerial distance of approximately 6.5 km within the megacaldera system of the Athesian Volcanic Group. Although substantial outcrops of sedimentary successions are missing between the two studied sections due to the erosion of the Etsch/Adige Valley, based on the extensive geological mappings we assume that the sections were deposited in the same sedimentary basin. The two sections cannot be stratigraphically correlated bed-by-bed, since there is a high lateral variation in facies, base and top of each outcrop are lithologically different reflecting a different sedimentation setting and rate. Both sections are a small part of a more or less extensive succession of predominantly coarse conglomerates without fossils. In addition, the

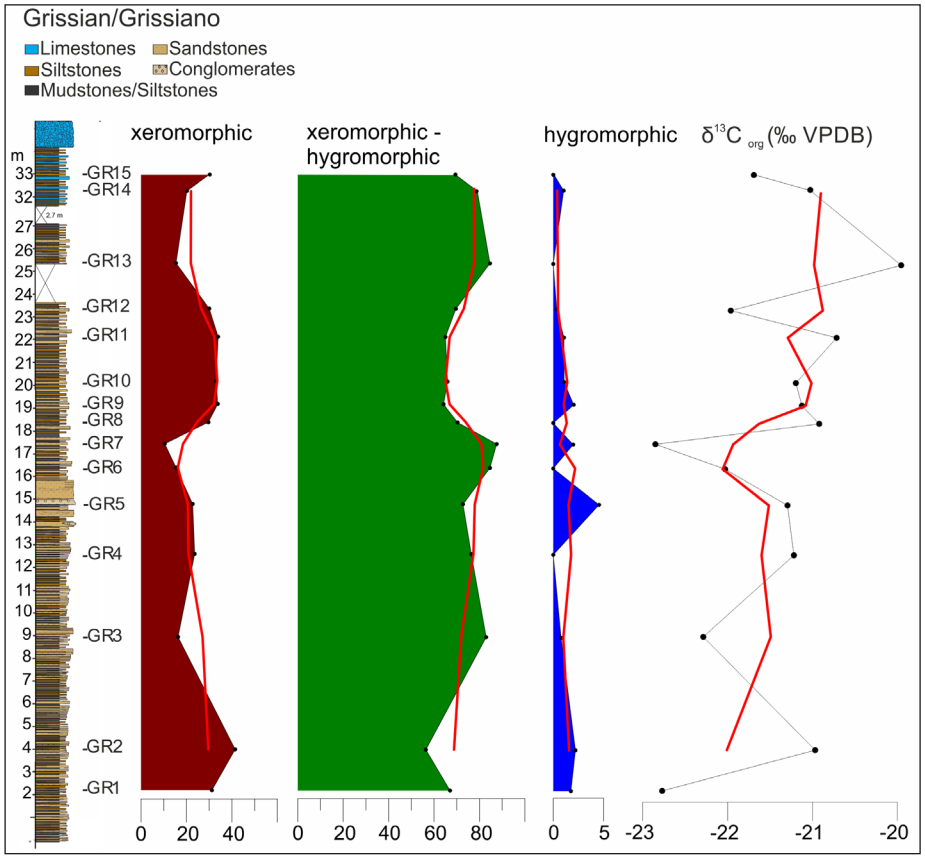

Fig. 14 - Ecoclimatic diagram of the Grissian/Grissiano section showing the relative percentages of the ecoclimatic affinities of the parent plants (xeromorphic, xeromorphic-hygromorphic, hygromorphic). Additionally, the $\delta^{13}C_{org}$ is also plotted. Red lines: 3-points moving average.

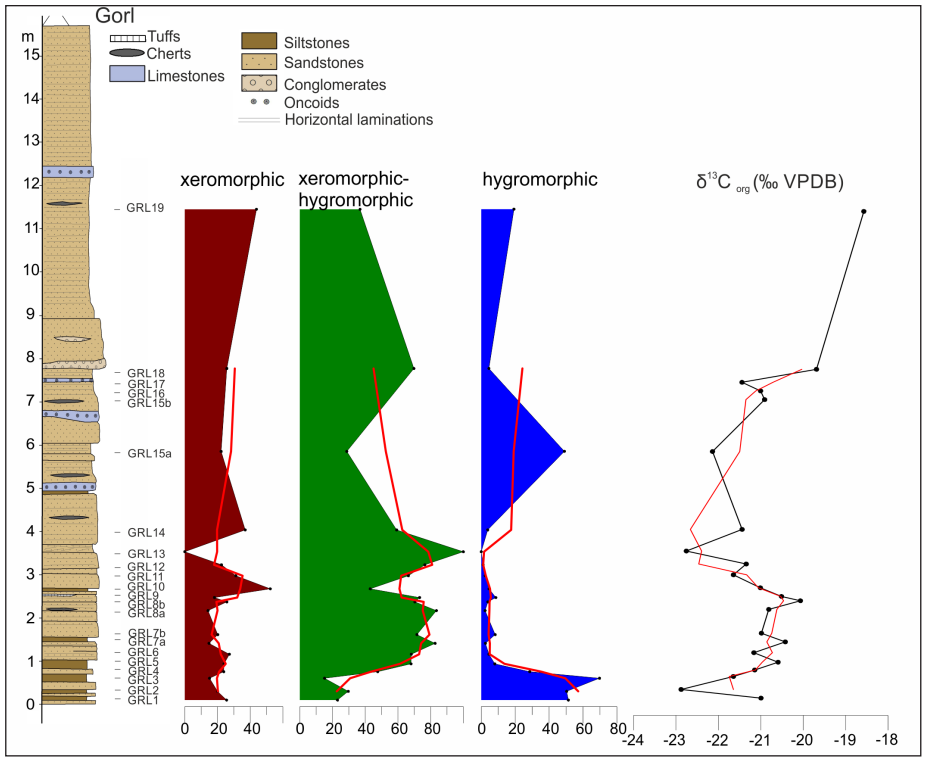

Fig. 15 - Ecoclimatic diagram of the Gorl section showing the relative percentages of the ecoclimatic affinities of the parent plants (xeromorphic, xeromorphic-hygromorphic, hygromorphic). Additionally, the $\delta^{13}C_{org}$ is also plotted. Red lines: 3-points moving average.

lack of organic matter in the conglomerates does not permit detailed correlation of the sections by stable carbon isotopes. Nonetheless, both sections represent the same stratigraphic record relating to a pause in eruptive activity, being under- and overlain by the same volcanic units (Avanzini et al. 2007; Bargossi et al. 2010).

Facies analyses

The lithofacies Gcm (clast-supported mas-

sive gravel) and Gmm (matrix-supported massive gravel) of the conglomeratic facies are interpreted as pseudoplastic and plastic debris flows and form the architectural element SG (sediment gravity flows) of Miall (1996, 2010). These debris flow deposits were formed in a proximal alluvial fan environment. Sandstones mostly belong to lithofacies Sh and Sm (horizontally laminated and massive sandstones) whereas lithofacies St and Sr (cross-bedded and ripple-laminated sandstones) occur only rarely. These lithofacies form the architectural element LS (laminated sand sheets) of Miall (1996, 2010). Laminated and massive sandstones are interpreted as sheetflood or flashflood deposits that formed on the distal part of alluvial fans or alluvial plains under upper flow-regime plane bed conditions. Lithofacies St and Sr are interpreted as fluvial deposits. Intercalated grain- and matrix-supported conglomerates represent distal debris flow deposits. Intercalated thin, commonly laminated siltstone beds (lithofacies Fl – laminated siltstones-mudstones – of Miall 1996, 2010) probably represent waning flood deposits.

Intercalated thin beds of (calcimicrobial) limestones, cherts, and oncolite beds in the Gorl section formed in a shallow lacustrine environment, indicating frequent flooding of distal alluvial fans and plains establishing a shallow lake. Freshwater oncoids occur in fluvial and lacustrine environments and are produced by cyanobacteria in association with green and red algae (Flügel 2010). In a lacustrine environment, oncoids are commonly concentrated in shallow, near shore settings with low water turbulence (Flügel 2010). Oncoids may be reworked during lowering of the lake level.

The limestones-cherts dominated facies in the Grissian/Grissiano section indicates a stable lake environment. Krainer & Spötl (1998) interpreted the irregular thin chert layers to have formed abiogenically in a physicochemical environment similar to that of modern Lake Magadi in the East African Rift Valley (Kenia). Precipitation of silica occurred as thin gel- or putty-like layers of hydrous Na-silicates. The three-dimensionally and well-preserved sporomorphs in the chert layers demonstrate that early-diagenetic lithification of the gel-like layers prevented compaction. Complex interbedding of limestones (including calcimicrobes), chert layers and thin, fine-grained siliciclastic sediments are probably caused by climatic fluctuations (drier and wetter periods) in a generally semiarid climate.

Architectural element SG (sediment gravity flows) represents the proximal alluvial fan facies. Sediment gravity flow deposits are characteristic on many modern alluvial fans in arid and semiarid regions (see Miall 1996). Basinward, the conglomeratic facies grades into the sandy facies representing the architectural element LS – laminated sand sheets, which formed by high-velocity flash floods on a distal alluvial fan or alluvial plain (sandflat), or rarely by fluvial processes.

Palynofacies and sporomorph analyses

The palynofacies assemblages of both Grissian/Grissiano and Gorl sections are mostly dominated by phytoclasts and sporomorphs (Figs. 9, 10 and Suppl. Figs. 1-2), suggesting a terrestrial origin. No freshwater algae such as *Botryococcus* were found.

There are some differences between the various samples and the two sections. To understand the origin of the similarities/dissimilarities between the 37 samples collected in the Grissian/Grissiano and Gorl sections, a PCA was performed with all samples in relation to the 14 main palynofacies variables (Fig. 16; Suppl. Tab. 3). The samples of Grissian/Grissiano and Gorl distribute in two different groups, mainly along the first axis (component 1) which explains 73.9 % of the total samples variance and mainly opposes the opaque equidimensional phytoclasts <50 μm to the well-preserved sporomorphs and the non-opaque phytoclasts (woody tissues, cuticles, and thin membranes with different degrees of preservation). Most of the Grissian/Grissiano samples show very negative scores (<20) along this axis, apart from GR4 with -13 and GR3 with -0.3, and GR5, GR6, GR13, which show positive scores and are placed closer to the Gorl samples GRL 4-7, 13, 15-17, 19, characterized by high abundance of opaque phytoclasts. A smaller part of the variance, ~13 %, is explained by the second axis (component 2). It separates Grissian/Grissiano samples GR14, GR15 and Gorl samples GRL3, GRL8a, GRL12, mainly relating to the different preservational states of their relatively abundant sporomorphs.

As the PCA (Fig. 16) and the calculated ratios (Figs. 9, 10) show, the Grissian/Grissiano and Gorl sections differ in the amount, shape and sizes of the opaque phytoclasts, in the composition and abundance of non-opaque phytoclasts, in the sporomorph abundances and preservation (see Com-

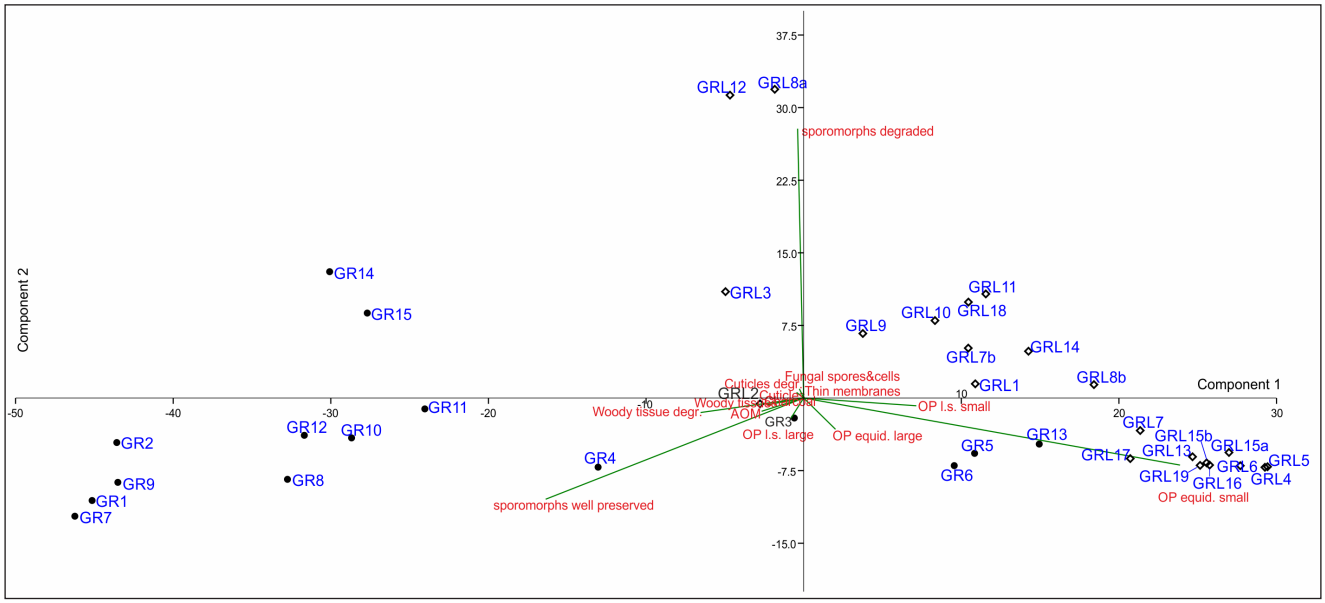

Fig. 16 - Biplot of the principal component analysis (PCA) showing the 37 palynological samples from Grissian/Grissiano (15 black dots) and Gorl (22 diamonds), as well as the 14 variables (indicated by the green lines and red characters).

ponent 2 in Fig. 16). To summarize the palynofacies composition and, thus, characterizing the local environmental conditions, a ternary plot was constructed (Fig. 17) according to the differences in the three most informative palynofacies categories: Abundance of sporomorphs, large phytoclasts (including both non-opaque and opaque phytoclasts) and small equidimensional opaque phytoclasts. Ternary plots are a commonly used tool in palynofacies analysis, but most existing variants are designed for marine environments (Tyson 1993, 1995; Aggarwal 2021 and references therein), although some authors modified them for continental settings (e.g., Aggarwal 2021 and references therein).

Generally, the opaque phytoclasts can derive from the oxidation of terrestrial woody materials during long transport in marine context, post-depositional degradation – for example due to seasonal changes of water level (Tyson 1993) – or from microbial activity. The black opaque equidimensional particles are the densest debris (McArthur et al. 2016). Their relatively high abundances could either reflect proximity to terrestrial sources (Wheeler et al. 2020; Aggarwal 2021) or reflect an intense microbial activity (Aggarwal 2021, and references therein). For the Gorl section, where sporomorph preservation is moderate to poor, the relatively higher opaque phytoclast percentages might be due to their higher preservation potential under oxidizing conditions or to their preferential concentration in sandy facies (Tyson 1993). Most of Gorl samples having the highest amount of equidimensional opaque phytoclasts < 50 µm (Figs. 10, 17, Suppl. Fig. 2) indicate a terrestrial depositional environment with relatively higher energy compared to Grissian/Grissiano and increased density sorting (Batten & Stead 2005).

In the Grissian/Grissiano section the assemblages contain abundant generally well-preserved sporomorphs, especially bisaccates (Figs. 9, 16 and Suppl. Fig. 1) that indicate a low-energy, more "distal" environment (Tyson 1993, 1995) in the relatively small and morphologically structured basin. For marine environments, Tyson & Follows (2000) demonstrated that the ratio of equidimensional to lath-shaped opaque phytoclasts can be used as a proxy of the distance between the site of deposition and the source of the continental sediments, where smaller values indicate a longer distance from the sediment sources. Here, this ratio was applied to reconstruct the distance of the source areas in a continental context (Figs. 9, 10) considering also the different lithofacies. Although both sections show similar ratio values, suggesting that no major changes in sediment supplies might have happened in both sections, the range of variation is slightly smaller in Gorl section than in Grissian/Grissiano section. In the Grissian/Grissiano section the ratio equidimensional to lath-shaped opaque phytoclasts decreases from 13 m upwards suggesting an in-

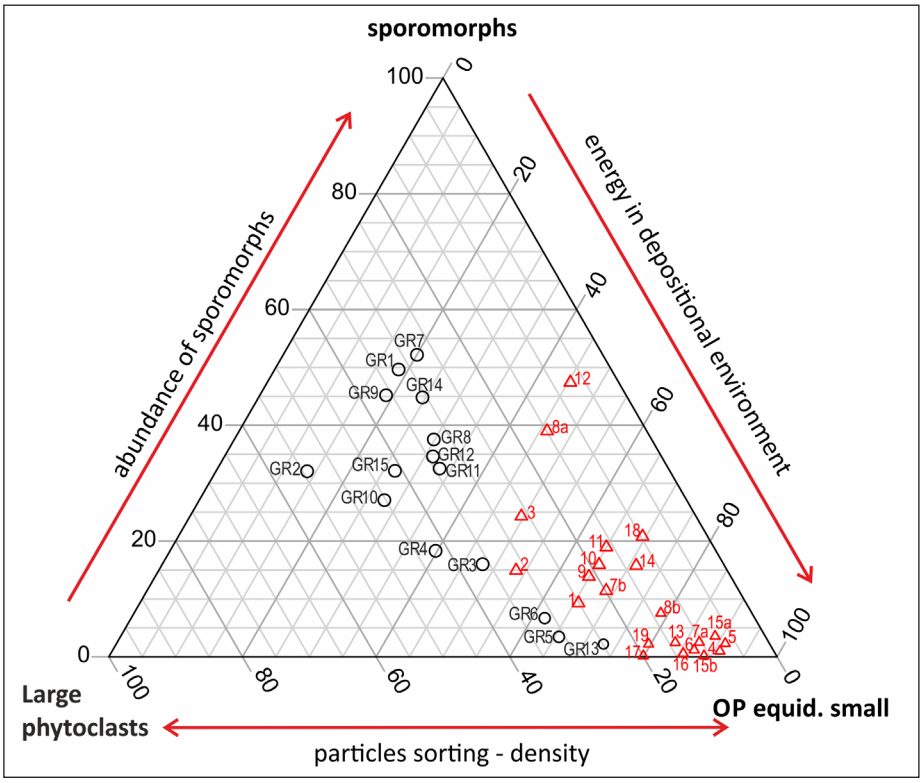

Fig. 17 - Ternary plot based on sporomorphs, small opaque phytoclasts (< 50 µm, mostly equidimensional = OP equid. small), and large phytoclasts (woody tissues, cuticles, opaque phytoclasts > 50 µm). Red triangles indicate the Gorl samples (1-19), black circles indicate the Grissian/Grissiano samples (GR1-GR15).

creasing distance from the sediment sources.

The first three samples of the Gorl section (GRL1-3) are distinct from the other GRL samples because they have high percentages in spores, partly degraded, from lycophytes and ferns (Tab. 2, Figs. 10, 13, Suppl. Fig. 2). They represent the hygromorphic plants living closer to the depositional site than the xeromorphic-hygromorphic and xeromorphic parent plants of saccate pollen. These samples might indicate a phase of recolonization by pioneer plants (Grauvogel-Stamm & Ash 2005) in an environment that was previously stressed by the high energy related to the deposition of conglomerates or a lateral change from alluvial fans to local depressions with wet soil and perhaps stagnant water close to the water body. After the first 4 m, the constant water-demanding plants were replaced by the ubiquitous more drought-tolerant xeromorphic-hygromorphic and xeromorphic vegetation.

Changes in water table levels at the Gorl site must have been more frequent than at the Grissian/Grissiano site. At Gorl, when the water table was low, oxidizing conditions must have occurred. This is suggested from the palynofacies assemblages, the absence of sporomorphs, and from the lithofacies (oncoids and carbonate layers).

In general, the Grissian/Grissiano palynofacies assemblages suggest a more stable environment and lower transport energy. The major change in the Grissian/Grissiano palynofacies assemblages is between 17 and 24 m (Fig. 9, Suppl. Fig. 1). No pronounced sedimentation changes are observed that could indicate alterations in the sedimentary input or lake level oscillations at that time, but an increase in the relative percentages of the xeromorphic taxa (Figs. 12, 14) suggests an expansion of these taxa near the depositional site.

The Grissian/Grissiano palynological records reflect more the xeromorphic vegetation living further from the water body (Figs. 14, 17, 18) while the Gorl site might be more influenced by the vegetation living closer to the water and the relative fluctuations of the lake level (Figs. 13, 15, 18). During short intervals, hygromorphic plants were growing close to the Gorl site representing a wet spot in an overall mixed forest of xeromorphic taxa (such as conifers, especially Voltziales) and xeromorphic-hygromorphic taxa (such as seed ferns, e.g., Peltaspermales). Spore-rich assemblages are rare in the Euramerican Cisuralian, and were restricted to small wet spots, while dominating saccates, especially taeniate bisaccates, derived from xeromorphic-hygromorphic and xeromorphic par-

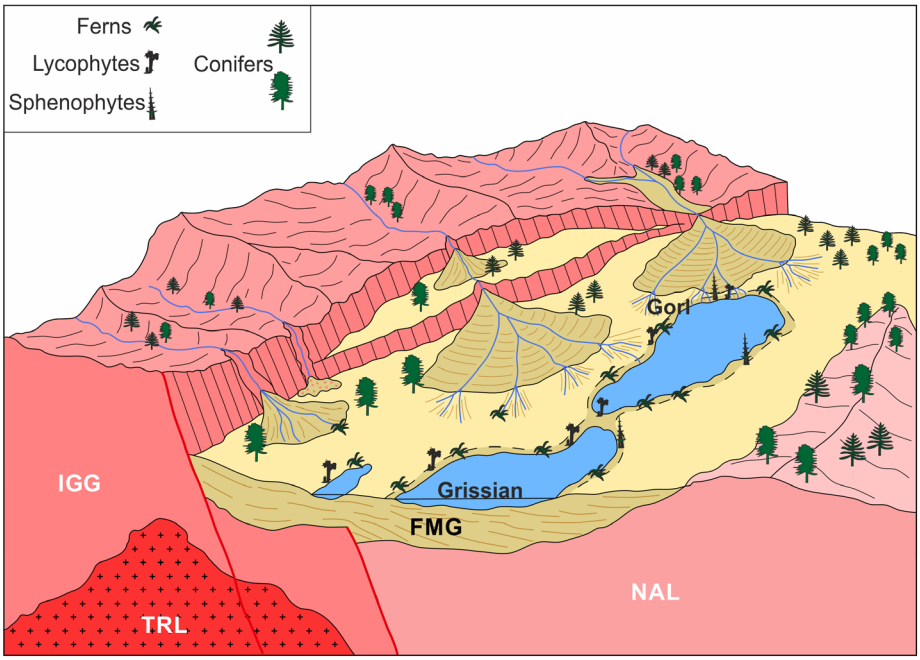

Fig. 18 - Interpretative sketch of the study area during the phase of sedimentary deposition in the Kungurian at the Grissian/Grissiano and Gorl sites. IGG - Gargazon/Gargazzone Formation, TRL - Terlan/Terlano Subvolcano body, NAL - Nals/Nalles Formation; FMG - Guntschna/Guncina Formation.

ent plants were ubiquitous. Such assemblages are well known and have been recorded e.g., from the Tregiovo Basin (Forte et al. 2018b) and the Lodève Basin (Doubinger et al. 1987).

Stable carbon isotopes and comparison with palynological data

The $\delta^{13}C_{org}$ of bulk rock from Gorl and Grissian/Grissiano has values between ca. -22.9 ‰ and -18.6 ‰, which are comparable with those of other Cisuralian continental organic matter and plants (e.g., Peters-Kottig et al. 2006; Forte et al. 2018b; Dong et al. 2021). Within this range, variations may be related to a change in the carbon isotope composition of atmospheric carbon, to local environmental factors such as water stress, to variations in provenance (e.g., a different taxonomic composition of plant fragments in the sample; or varying proportions in the type of organic matter), or even to differential diagenesis. Some of these factors may be excluded, because of the shortness of the investigated succession. Given the short time that is represented, it is unlikely that the Permian $\delta^{13}C_{org}$ trends were captured here. Likewise, it is improbable that samples collected within a few metres underwent such differential burial as to determine differences in the diagenesis of organic matter. It is instead more likely that isotopic variability in bulk samples represents either quick changes in the local environment, and/or changes in the provenance of organic matter. To investigate this possibility, the $\delta^{13}C_{org}$ of bulk rock samples was compared to the palynological compositions. Little correlation between the isotope records and the three ecoclimatic components (xeromorphic, xeromorphic-hygromorphic and hygromorphic taxa) has been observed in the Grissian/Grissiano or Gorl sections. Nevertheless, considering all Grissian/Grissiano and Gorl samples as a whole we found a weak but significant positive correlation ($r=0.35$, at $p<0.05$) between xeromorphic taxa and the $\delta^{13}C_{org}$ values. Therefore, a small part of the variability of $\delta^{13}C_{org}$ values may be explained by the ecological preference of the plants contributing to the organic carbon preserved in the sedimentary rocks.

Reconstruction of the depositional environments

The sedimentary successions of Grissian/Grissiano and Gorl belong to the Guntschna/Guncina Formation and were deposited in the same sedimentary basin that was formed by a volcano-tectonic collapse related to a resurgent dome (Morelli et al. 2012). The unit reaches its maximum thickness (up to 250 m) near the northern marginal fault running from Terlan/Terlano to Bozen/Bolzano (Figs. 2, 3). The original size and shape of the sedimentary basin can be inferred from outcrops present on both flanks of the Etsch/Adige valley. The basin was probably elongate and oriented parallel to the collapse in a WNW-ESE direction with a minimum length of at least 15-20 km and

a maximum width of about 6 km. The basin was probably subdivided into more or less communicating sub-basins depending on the palaeotopography formed by the collapse and subsequent volcanic eruptions (Fig. 18).

Coarse-grained alluvial fan sediments are dominant at the base of the succession and near the northern margin of the basin, grading into fine-grained alluvial fan and sandflat sediments towards the top and the centre. Lacustrine sediments are present only in the upper part of the succession and located in the area between Terlan/Terlano and Grissian/Grissiano.

Sedimentation took place during a period without significant volcanic eruptions and under predominantly semiarid climatic conditions, although periods with drier and wetter climate occurred, as documented by the alternation of limestone and chert layers in the uppermost part of the lacustrine facies at Grissian/Grissiano.

The sedimentary successions of both locations show a clear vertical and lateral trend from proximal, coarse-grained alluvial fan deposits to distal alluvial fan and sandflat sediments and finally to lacustrine deposits. The clastic sediments of the Guntschna/Guncina Formation are derived mostly from eroded volcanic rocks of the Gargazon/Gargazzone Formation outcropping to the north.

The sedimentary succession of Gorl represents a more marginal facies of the basin, characterized by a sandstone-dominated facies of a sandflat environment with intercalated thin lacustrine deposits. These thin lacustrine sediments are composed of fine-grained siliciclastics, interbedded limestones formed partly by cyanobacteria (calcimicrobes) and chert layers. At Grissian/Grissiano the more basinal facies is exposed with a shallow lacustrine environment (Fig. 18) composed of alternating limestone and chert layers at the top of the succession that persisted over a longer period.

Conclusions

The megacaldera system of the Athesian Volcanic Group (South Tyrol, N-Italy) is an outstanding succession of alternating volcanic and sedimentary rocks covering ~15 Myr of the late Cisuralian. The multidisciplinary study of lithofacies, palynofacies, sporomorphs and stable carbon isotopes of two sedimentary successions gives insights into a complex Kungurian tropical landscape. The two sedimentary successions of Grissian/Grissiano and Gorl, located only a few kilometers apart, correspond to the same quiescent phase of the volcanic activity, which has a maximum estimated duration of approximately 2.1 million years. The Guntschna/Guncina Formation records the depositional environment inside the megacaldera: it was dominated by fans with predominantly sandstones and conglomerates evolving on top into subordinate lacustrine areas, probably subdivided into several more or less communicating basins with shallow water bodies influenced by the palaeotopography.

The Gorl succession was deposited at the margin of a water body located in a marginal position of the sedimentary basin and characterized by high water energy. The palynological content near the base of the Gorl succession (GRL1-3) is represented by a relatively high percentage of spores deriving from lycophytes and ferns. This is interpreted as a phase of recolonization by pioneer plants, after a high-energy erosional phase, probably caused by the active volcanism or volcano-tectonics, as evidenced by the deposition of massive conglomerates at the base of the sedimentary succession. The stratigraphic succession of Grissian/Grissiano has been deposited in the more distal area of a shallow lacustrine environment with low energy and more stable environmental conditions. The difference in the organic particle assemblages between the two outcrops is mostly linked to the distance from the margin of the lake and energy during the deposition of the sediments. Grissian/Grissiano, the section that is in a more distal position, is less influenced by the smaller environmental disruptions that are more distinct and easier to observe in the more marginal succession of Gorl.

Sporomorph assemblages show that the plant communities of the megacaldera were dominated by xeromorphic elements such as conifers. Pollen of other gymnosperm groups, adapted to arid or semiarid conditions like seed ferns, are also very abundant. Hygromorphic elements like lycophytes and ferns, on the other hand, were rare and distributed mainly close to the margin of the lakes. A general semiarid climate with several minor spells of local drier and wetter conditions is reconstructed by the various proxies such as geochemis-

try and palynology, in agreement with the stepwise aridification trend that started in the Pennsylvanian (e.g., Roscher & Schneider 2006; DiMichele et al. 2008, 2009; Bashforth et al. 2021). The climatic fluctuations are only observed in the marginal facies of Gorl, underscoring how sensitive these marginal lake environments were also to minor climatic shifts. The Grissian/Grissiano succession is more buffered due to its greater distance from the lake margin and the lower transport energy. The differences between the two successions, as well as the relatively stable carbon isotope record at Grissian/Grissiano and Gorl show that the shifts observed in Gorl are only of local scale.

This study shows how sensitive the terrestrial successions of the Athesian Volcanic Group were as they recorded regional and local changes in the environment and climate. Future works will integrate the present study with other sections in the megacaldera, thus extending its chronostratigraphic range, by applying the same integrated approach to several outcropping successions distributed in different time intervals and geographic settings of the megacaldera system. This will allow us to reconstruct the development of the depositional and palaeoenvironmental systems in this unique setting during the 15 Myr of volcanic activity. In addition, the studies will contribute to the knowledge of the terrestrial environments of the Cisuralian in eastern equatorial Pangea, in particular their evolution in relation to the volcanic activity. Further considerations about the impact that the super-eruptions of the Athesian Volcanic Group had on the climate and developing ecosystems may be possible through comparisons with the more recent super-eruptions that formed the megacalderas of Yellowstone, USA and Toba, Indonesia (Miller & Wark 2008).

Acknowledgements: The Editor Lucia Angiolini, Amalia Spina and an anonymous reviewer are gratefully acknowledged for their constructive comments. This research is part of the project "Living with the supervolcano - How Athesian eruptions destroyed and preserved 15 million years of Permian life" financed by the Promotion of Educational Policies, University and Research Department of the Autonomous Province of Bolzano — South Tyrol nr. 11/34.

References

Aggarwal N. (2021) - Sedimentary organic matter as a proficient tool for the palaeoenvironmental and palaeodepositional settings on Gondwana coal deposits. *Journal of Petroleum Exploration and Production Technology*. https://doi.org/10.1007/s13202-021-01331-x.

Aspmair C. & Krainer K. (1998) - Fossile Pflanzenreste in Seeablagerungen der Bozner Quarzporphyrabfolge des mittleren Etschtales (Südtirol) und ihre Bedeutung für das Klima im Perm der Südalpen. *Der Schlern*, 45(4): 245-260.

Avanzini M., Bargossi G.M., Borsato A, Castiglioni G.B., Cucato M., Morelli C., Prosser G. & Sapelza A. (2007) - Note Illustrative della Carta Geologica d'Italia alla Scala 1:50.000, Foglio 026, APPIANO. Servizio Geologico d'Italia, Roma, 192 pp.

Avanzini M., Contardi P., Ronchi A. & Santi G. (2011) - Ichnosystematics of the Lower Permian invertebrate traces from the Collio and Mt. Luco Basins (North Italy). *Ichnos,* 18: 95-11.

Bargossi G.M., Bove G., Cucato M., Gregnanin A., Morelli C., Moretti A., Poli S., Zanchetta S. & Zanchi A. (2010) - Note Illustrative della Carta Geologica d'Italia alla Scala 1:50.000. Foglio 013, MERANO. ISPRA, Servizio Geologico d'Italia, Roma, 314 pp.

Barth S. & Mohr B.A. (1994) - Palynostratigraphically determined age of the Tregiovo sedimentary complex in relation to radiometric emplacement ages of the Athesian volcanic complex (Permian, Southern Alps, N Italy). *Neues Jahrbuch für Geologie und Paläontologie Abhandlungen*, 192(2): 273-292.

Bashforth A.R., DiMichele W.A., Eble C.F., Falcon-Lang H.J., Looy C.V. & Lucas S.G. (2021) - The environmental implications of upper Paleozoic plant-fossil assemblages with mixtures of wetland and drought-tolerant taxa in tropical Pangea. *Geobios*, 68: 1-45.

Batten D.J. (1996) - Chapter 26A. Palynofacies and palaeoenvironmental interpretation. In: Jansonius J. & McGregor D.C (Eds) - Palynology: principles and applications; 3: 1011-1064. American Association of Stratigraphic Palynologists Foundation.

Batten D.J. & Stead D.T. (2005) - Palynofacies Analysis and Its Stratigraphic Application. In: Koutsoukos E.A.M. (Ed.) - Applied Stratigraphy: 203-226, Springer.

Brandner R., Gruber A., Morelli C. & Mair V. (2016) - Pulses of Neotethys - rifting in the Permomesozoic of the Dolomites. *Geo. Alp*, 13: 7-69.

Cassinis G. & Neri C. (1992) - Sedimentary and paleotectonic evolution of some Permian continental basins in the central Southern Alps, Italy. In: Courel, L. and Ramos, A. (Eds), Continental Permian in Europe. *Cuadernos de Geología Ibérica*, 16: 145-176.

Cassinis G. & Doubinger J. (1991) - On the geological time of the typical Collio and Tregiovo continental beds in the Southalpine Permian (Italy), and some additional observations. *Atti Ticinensi di Scienze della Terra*, 34: 1-20.

Cassinis G. & Doubinger J. (1992) - Artinskian to Ufimian palynomorph assemblages from the Central Southern Alps, Italy and their regional stratigraphic implications. In: Nairn A.E.M. & Koroteev V. (Eds) - Contributions to Eurasian Geology, Papers Presented at the International Congress Permian System of the World, Part I: 9-18. University of South Carolina, Columbia.

Cirilli S., Panfili G., Buratti N. & Frixa A. (2018) - Paleoenvi-

ronmental reconstruction by means of palynofacies and lithofacies analyses: An example from the Upper Triassic subsurface succession of the Hyblean Plateau Petroleum System (SE Sicily, Italy). *Review of Palaeobotany and Palynology*, 253: 70-87.

DiMichele W.A., Kerp H., Tabor N.J. & Looy C.V. (2008) - The so-called "Paleophytic-Mesophytic" transition in equatorial Pangea - multiple biomes and vegetational tracking of climate change through geological time. *Palaeogeography, Palaeoclimatology, Palaeoecology*, 268: 152-163.

DiMichele W.A., Montañez I.P., Poulsen C.J. & Tabor N.J. (2009) - Climate and vegetational regime shifts in the late Paleozoic ice age earth. *Geobiology*, 7(2): 200-226.

Dong Y., Cui Y., Wang J., Chen H., Zhang F., Wu Y., Li Z., Zhu P. & Jiang S. (2021) - Paleozoic carbon cycle dynamics: Insights from stable carbon isotopes in marine carbonates and C_3 land plants. *Earth-Science Reviews*, 222: 103813.

Doubinger J., Odin B. & Conrad G. (1987) - Les associations sporopolliniques du Permien continental du bassin de Lodève (Hérault, France): caractérisation de l'Autunien supérieur, du 'Saxonien' et du Thuringien. *Annales de la Société Géologique du Nord*, 106: 103-109.

Fels H. & Paul-Koch G. (1985) - Alluviale Schüttungsfächer innerhalb der unterpermischen Vulkanite Südtirols (Italien). *Zeitschrift der deutschen geologischen Gesellschaft*, 136: 167-179.

Flügel E. (2010) - Microfacies of Carbonate Rocks. Analysis, Interpretation and Application. Second Edition - Springer-Verlag, Berlin, 984 pp.

Forte G., Kustatscher E., van Konijnenburg-van Cittert J.H.A., Looy C.V. & Kerp H. (2017) - Conifer diversity in the Kungurian of Europe – Evidence from dwarf-shoot morphology. *Review of Palaeobotany and Palynology*, 244: 308-315.

Forte G., Kustatscher E., van Konijnenburg-van Cittert J.H.A. & Kerp H. (2018a) - Sphenopterid diversity in the Kungurian of Tregiovo (Trento, NE-Italy). *Review of Palaeobotany and Palynology*, 252: 64-76.

Forte G., Kustatscher E., Roghi G. & Preto N. (2018b) - The Permian (Kungurian, Cisuralian) palaeoenvironment and palaeoclimate of the Tregiovo Basin, Italy: Palaeobotanical, palynological and geochemical investigations. *Palaeogeography, Palaeoclimatology, Palaeoecology*, 495: 186-204.

Frakes L.A., Francis J.E. & Syktus J.I. (1992) - Climate modes of the Phanerozoic. New York: Cambridge University Press, 274 pp.

Giannotti G.P. (1962) - Intercalazioni lacustri entro le vulcaniti paleozoiche atesine. *Atti Società Toscana Scienze Naturali*, 2: 3-22.

Grauvogel-Stamm L. & Ash S.R. (2005) - Recovery of the Triassic land flora from the end-Permian life crisis. *Comptes Rendus Palevol.*, 4(6-7): 593-608.

Hammer Ø., Harper D.T.A & Ryan P.D. (2001) - PAST: Paleontological Statistics software package for education and data analysis. *Palaeontologia Electronica*, 4(1): 9 pp.

Hartkopf-Fröder C., Wood G.D. & Krainer K. (2001) - Palynology of the Permian Bolzano Volcanic Complex, Southern Alps, Italy, Part 1: Miospore preservation, quantitative spore color and quantitative fluorescence microscopy. In: Goodman D.K. & Clarke R.T. (Eds) - Proceedings of the IX International Palynological Congress, Houston, Texas, U.S.A., 1996: 79-97. American Association of Stratigraphic Palynologists Foundation.

Isbell J.L., Miller M.F., Wolfe K.L. & Lenaker P.A. (2003) - Timing of late Paleozoic glaciation in Gondwana: Was glaciation responsible of the development of northern hemisphere cyclothems? In: Chan M.A., Archer A.W. (Eds) - Extreme Depositional Environments: Mega End Members in Geologic Time. *Geological Society of America, Special Paper*, 370: 5-24.

Isbell J.L., Vesely F.F., Rosa E.L.M., Pauls K.N., Fedorchuk N.D., Ives L.R.W., McNall N.B., Litwin S.A., Borucki M.K., Malone J.E. & Kusick A.R. (2021) - Evaluation of physical and chemical proxies used to interpret past glaciations with a focus on the late Paleozoic Ice Age. *Earth-Science Reviews*, 221: 103756.

Jones A.T. & Fielding C.R. (2004) - Sedimentological record of the late Paleozoic glaciation in Queensland, Australia. *Geology*, 32: 153-156.

Krainer K. & Spötl C. (1998) - Abiogenic silica layers within a fluvio-lacustrine succession, Bolzano Volcanic Complex, northern Italy: a Permian analogue for Magadi-type cherts? *Sedimentology*, 45: 489-505.

Marchetti L., Forte G., Bernardi M., Wappler T., Hartkopf-Fröder C., Krainer K. & Kustatscher E. (2015) - Reconstruction of a Late Cisuralian (Early Permian) floodplain lake environment: Palaeontology and sedimentology of the Tregiovo Basin (Trentino-Alto Adige, Northern Italy). *Palaeogeography, Palaeoclimatology, Palaeoecology*, 440: 180-200.

Marchetti L., Tessarollo A., Felletti F. & Ronchi A. (2017) - Tetrapod footprint paleoecology: behavior, taphonomy and ichnofauna disentangled. A case study from the Lower Permian of the Southern Alps (Italy). *Palaios*, 32: 506-527.

Marchetti L., Forte G., Kustatscher E., DiMichele W.A., Spencer L., Roghi G., Juncal M., Hartkopf-Fröder C., Krainer K., Morelli C. & Ronchi A. (2022) - The Artinskian Warming Event: an Euramerican change in climate and the terrestrial biota during the early Permian. *Earth-Science Reviews*, 226: 103922.

Marocchi M., Morelli C., Klötzli U. & Bargossi G.M (2008) - Evolution of large silicic magma systems: New U-Pb Zircon data on the NW Permian Athesian Volcanic Group (Southern Alps, Italy). *The Journal of Geology*, 116: 480-498.

Martín-Closas C., Permanyer A. & Vila M.J. (2005) - Palynofacies distribution in a lacustrine basin. *Geobios*, 38:197-210.

McArthur A.D., Kneller B.C., Wakefield M.I., Souza P.A. & Kuchle J. (2016) - Palynofacies classification of the depositional elements of confined turbidite systems: Examples from the Gres d'Annot, SE France. *Marine and Petroleum Geology*, 77: 1254-1273.

Miall A.D. (1996) - The Geology of Fluvial Deposits. Sedimentary Facies, Basin Analysis, and Petroleum Geology. -Springer-Verlag, Berlin, 582 pp.

Miall A.D. (2010) - Alluvial Deposits. In: James N.P. & Dalrymple R.W. (Eds) - Facies Models 4: 105-137. Geological Association of Canada.

Miller C.F. & Wark D.A. (2008) - Supervolcanoes and their explosive supereruptions. *Elements*, 4: 11-16.

Montañez I.P., Tabor N.J., Niemeier D., DiMichele W.A., Frank T.D., Fielding C.R., Isbell J.L., Birgenheier L.T. & Rygel M. (2007) - CO_2-forced climate and vegetation instability during Late Paleozoic glaciation. *Science*, 315: 87-91.

Montañez I.P. & Poulsen C.J. (2013) - The Late Paleozoic ice age: an evolving paradigm. *Annual Review of Earth and Planetary Sciences*, 41: 629-656.

Montañez I.P., McElwain J.C., Poulsen C.J., White J.D., DiMichele W.A., Wilson J.P., Griggs G. & Hren M.T. (2016) - Climate, pCO_2 and terrestrial carbon cycle linkages during late Palaeozoic glacial-interglacial cycles. *Nature Geoscience*, 9: 824-828.

Montañez I.P. (2022) - Current synthesis of the penultimate icehouse and its imprint on the Upper Devonian through Permian stratigraphic record. *Geological Society of London, Special Publication*, 512: 213-245.

Morelli C., Bargossi G.M., Mair V., Marocchi M. & Moretti A. (2007) - The lower Permian volcanics along the Etsch valley from Meran to Auer (Bozen). *Mitteilungen der österreichischen mineralogischen Gesellschaft*, 153: 195-218.

Morelli C., Marocchi M., Moretti A., Bargossi G.M., Gasparotto G., De Waele B., Klötzli U. & Mair V. (2012) - Volcanic stratigraphy and radiometric age constrains at the northern margin of a mega-caldera system: Athesian Volcanic Group (Southern Alps, Italy). *GeoActa*, 11: 51-67. Bologna.

Müller A.B., Strauss H., Hartkopf-Fröder C. & Littke R. (2006) - Reconstructing the evolution of the latest Pennsylvanian-earliest Permian lake Odernheim based on stable isotope geochemistry and palynofacies: a case study from the Saar-Nahe Basin, Germany. *Palaeogeography, Palaeoclimatology, Palaeoecology*, 240: 204-224.

Neri C., Avanzini M., Bampi T., Bargossi G.M., Mair V., Morelli C., Pittau P., Rochi A. & Sapelza A. (1999) - The Tregiovo area and related volcanics in the Tregiovo section. In: Cassinis, G., Cortesogno, L., Gagger, L., Massari, F., Neri, C., Nicosia, U., Pittau, P. (Eds), Stratigraphy and facies of the Permian deposits between eastern Lombardy and western Dolomites, Field Trip Guide (Appendix): 81-89. Pavia University, Earth Sciences Department.

Olszewski T.D. & Patzkowsky M.E. (2003) - From cyclothems to sequences: the record of eustasy and climate on an icehouse epeiric platform (Pennsylvanian-Permian, North American Midcontinent). *Journal of Sedimentary Research*, 73(1): 15-30.

Peters-Kottig W., Strauss H. & Kerp H. (2006) - The land plant $\delta^{13}C$ record and plant evolution in the Late Palaeozoic. *Palaeogeography, Palaeoclimatology, Palaeoecology*, 240: 237-252.

R Core Team (2021) - R: A language and environment for statistical computing. R Foundation for Statistical Computing, Vienna, Austria. URL https://www.R-project.org/.

Rankey E.C. (1997) - Relations between relative changes in sea level and climate shifts: Pennsylvanian - Permian mixed carbonate-siliciclastic strata, western United States. *Geological Society of America Bulletin,* 109: 1089-1100.

Roscher M. & Schneider J.W. (2006) - Permo-Carboniferous climate: Early Pennsylvanian to Late Permian climate development of central Europe in a regional and global context. *Geological Society London, Special Publication*, 265: 95-136.

Schaltegger U. & Brack P. (2007) - Crustal-scale magmatic systems during intracontinental strike-slip tectonics: U, Pb and Hf isotopic constraints from Permian magmatic rocks of the Southern Alps. *International Journal of Earth Sciences* (*Geol. Rundsch.*), 96: 1131-1151.

Schneider J.W., Körner F., Roscher M. & Kroner U. (2006) - Permian climate development in the northern peri-Tethys area – The Lodève Basin, French Massif Central, compared in a European and global context. *Palaeogeography, Palaeoclimatology, Palaeoecology*, 240: 161-183.

Schneider J.W., Lucas S.G., Scholze F., Voigt S., Marchetti L., Opluštil S., Werneburg R., Golubev V., Barrick J.E., Nemyrovska T., Ronchi A., Silantiev V., Rößler R., Saber H., Linnemann U., Zarinova V. & Shen S. (2020) - Late Paleozoic - early Mesozoic continental biostratigraphy - links to the Standard Global Chronostratigraphic Scale. *Palaeoworld,* 29: 186-238.

Smith M.R. (2017) - Ternary: An R Package for Creating Ternary Plots. *Comprehensive R Archive Network*.

Spina A., Cirilli S., Sorci A., Schito A., Clayton G., Corrado S., Fernandes P., Galasso F., Montesi G., Pereira Z., Rashidi M. & Rettori R. (2021) - Assessing thermal maturity through a Multi-Proxy Approach: A Case Study from the Permian Faraghan Formation (Zagros Basin, Southwest Iran). *Geosciences*, 11: 484.

Tyson R.V. (1993) - Palynofacies analysis. In: Jenkins D.G. (Ed.) - Applied Micropalaeontology: 153-191. Kluwer, Dordrecht.

Tyson R.V. (1995) - Sedimentary organic matter: organic facies and palynofacies. Springer Science and Business Media, 615 pp.

Tyson R.V. & Follows B. (2000) - Palynofacies prediction of distance from sediment source: A case study from the Upper Cretaceous of the Pyrenees. *Geology*, 28(6): 569-571.

Visscher H., Kerp H., Clement-Westerhof J.A. & Looy C. (2001) - Permian floras of the Southern Alps. *Natura Bresciana, Museo Civico di Scienze Naturali, Brescia, Monografia*, 25: 117-123.

Visonà D., Fioretti A.M., Poli M.E., Zanferrari A. & Fanning M. (2007) - U-Pb SHRIMP zircon dating of andesite from the Dolomite area (NE Italy): geochronological evidence for the early onset of Permian volcanism in the eastern part of the Southern Alps. *Swiss Journal of Geosciences*, 100: 313-324.

Wheeler A., Van de Wetering N., Esterle J.S. & Götz A.E. (2020) - Palaeoenvironmental changes recorded in the palynology and palynofacies of a Late Permian Marker Mudstone (Galilee Basin, Australia). *Palaeoworld*, 29: 439-452.